GRABBING ROCK IN DEEP SEA MINING

THE EFFECT OF OFFERING NATURAL FORCE FEEDBACK AND HAPTIC SHARED CONTROL ON RATE AND FORCE CONTROL OF A DEEP SEA MINING SUSPENDED GRAB

R.J. Kuiper

Delft, 15th of February 2012

SECTION: MECHANICAL ENGINEERING
SPECIALIZATION: BIOMECHANICAL DESIGN
STUDENT NO.: 1175408

TU Delft Delft University of Technology

seatools

Prof.dr. F.C.T. van der Helm *(ME)*
Dr.ir. D.A. Abbink *(ME)*

Ir. J.C.L. Frumau
Ir. S. Tamsma

Copyright © 2012 by Seatools bv.

All rights reserved. Complying with all applicable copyright laws is the responsibility of the user. No part of this document may be reproduced, stored in a retrieval system, or transmitted in any form or by any means, electronic, mechanical, photocopying, recording, or otherwise, without express written permission of Seatools bv.

If, however, your only means of access is electronic, permission to print one copy is hereby granted.

In no event will Seatools bv. or its employees be liable for any consequential, incidental or indirect damages (including damages for loss of business profits or business information, business interruption, and the like), arising out the use of or inability to use this document, even if Seatools bv. has been advised of the possibility of such damages.

Information in this document is subject to change without notice.

PREFACE

I have accomplished a double master degree at the Delft University of Technology, one for Mechanical Engineering and one for Offshore and Dredging Engineering. This document describes the thesis part for my Mechanical Engineering master with the specialisation Biomechanical Design, which focused on the design and evaluation of different feedback mechanisms to control a suspended grab for excavating rock in a deep sea mining process. This document is written according to the agreement between Seatools bv. and the Delft University of Technology. The confidential information is removed from this document and this version is only for publicly access in the digital archives of Delft University of Technology. More detailed information of the experimental results and design details is accessible by contacting Seatools bv.

This document is written with the support of David Abbink, Jan Frumau and Frans van der Helm through several discussions guiding the thesis and constructing feedback of the draft report. Great support for conducting the experiments is given to me from Sieds Tamsma and David Abbink. Both the TU Delft and Seatools bv. greatly supported the research with materials and knowledge.

ABSTRACT

High concentrations of common and rare-earth metals are found on the seafloor in rock material named seafloor massive sulphides deposits, at depths up to 2000 meters. A proposition for excavating these deposits at such great depths is to use a large suspended grab, controlled by teleoperation. Such a mining operation has as goal to excavate the maximum amount of minerals at the minimal amount of time. Environmental uncertainties prohibit the use of full automation, inducing the need of an operator controlling the process by teleoperation. General problems that are expected to occur with teleoperation of a large machine on great depths are operator's performance and situation awareness, which can reduce operational efficiency and might even lead to failure when not undertaking appropriate responses in critical situations. Therefore optimization of the grasping teleoperation is needed to increase the entire excavation performance and decrease periods of operational downtime due to incorrect execution of the operator.

Two approaches from literature seem promising for improving the human-machine interface of remote grasping: 'natural force feedback' (i.e., reflecting system forces to the operator during grasping, creating transparency in the teleoperation), or 'haptic shared control' (i.e., sharing the control through forces on the input device, therefore guiding the operator based on constraints in the environment). Natural force feedback has been shown in literature to increase situation awareness and performance of a teleoperation by reflecting information of the environment to the operator. Forces of the hydraulic actuators for excavating rock material with a grab are used for natural feedback to the operator. Haptic shared control is shown to increase task performance and decrease control effort of a teleoperation with position control. Artificial forces are used to guide the operator to control the process efficiently and prevent incorrect responses in critical situations. Combining natural force feedback and haptic shared control could be an optimal solution to increase grasping performance on a deep sea mining teleoperation.

The goal of this thesis is to determine the improvements for the operator using these two feedback mechanisms for controlling a deep sea mining grabbing process. An experimental setup has been developed to validate the hypotheses of improved performance and situation awareness using haptic feedback. The experimental setup consists of two joysticks for controlling the velocity and force of the hoisting cable and clamshells of the simulated process, based on a comparable dredging application. A visual projection of the process is displayed to the operator, with additional visual information such as position and forces of the hoisting cable and clamshells, for optimal control of the process. Both haptic feedback mechanisms are applied separately and combined as experimental conditions during the experiment and compared with a baseline condition without haptic feedback. The experiments are conducted using two types of trials: 'performance trials' (i.e., trials conducted at normal operational conditions) and 'catch trials' (i.e., trials at difficult conditions which cannot always be fully completed), to determine improvements in excavation production, control effort and responses in critical situations.

The experimental results for performance trials showed no improvements in performance, neither offering natural force feedback as haptic shared control, based on excavation production results. Haptic shared control however did show a reduction of control effort during performance trials, based on total summation angles of control inputs and subjective workload. When offering natural force feedback, reduction of control effort only occurred when it was combined with haptic shared control. Natural force feedback indicated an increase of situation awareness based on reduction of the maximal heeling angle of the machine at ground contact, preventing the machine to fall over during catch trials. When offering haptic shared control, a reduction of heeling angle only occurred when also offering natural force feedback. This implies that natural force feedback improved the situation awareness at critical situations, resulting in less production loss and damaging of the system. Haptic shared control on the other hand reduced the control effort, resulting in an increased attention of the operator during the entire process, due to a less demanding task.

CONTENTS

1 INTRODUCTION

New technologies such as mobile phones and laptops are rapidly increasing the demand for rare-earth metals such as tellurium, selenium and rubidium. Also the prizes are rising for common metals such as gold, silver and copper. This induces the need to look for new material resources. A solution for new material resources is found by collecting deposits on the seafloor at depths of 2000m, through a process called deep sea mining. Excavating these deposits from the seafloor is a challenging task, due to large depth and high costs of such a process resulting in the need for a large production rate. A promising option for excavating mineral deposits is the use of a suspended grab. Full autonomous operation is not feasible due to several factors, such as unknown reactions of rock sediments in deep waters and positioning uncertainties. The human operator therefore needs to be included in the process, which requires an intuitive human-machine interface in order to control the excavation process by teleoperation. A description of a deep sea mining process with a suspended grab for excavating rock materials is given in paragraph 1.1. The general principle of teleoperation and two haptic feedback mechanisms as found in literature is described in paragraph 1.2. The difference of a grasping teleoperation as used for controlling a suspended grab is described in paragraph 1.3. Paragraph 1.4 describes the problem statement for this thesis, paragraph 1.5 the hypothesis and paragraph 1.6 the approach of this thesis to verify the hypothesis.

1.1 Deep Sea Mining Process Description

An overview of a deep sea mining process using a suspended grab is given in paragraph 1.1.1 and the main control parameters in paragraph 1.1.2. Paragraph 1.1.3 gives a brief overview of the principle of a hydraulic actuator and the transition of force and velocity of such a system. A decomposition of an entire deep sea mining task is given in paragraph 1.1.4.

1.1.1 Situation Overview

Excavation of rock material from the seafloor for a deep sea mining process is a large technical difficulty due to the size and forces of the process. The production has to be large scale due to the offshore location and therefore costs of such a process. Due to this scale, the size of machinery and encountered forces are large and difficult to operate. A promising way for excavation is the use of a large hydraulic grab, suspended from a ship with a hoisting cable as shown in Figure 1. The grab can translate in horizontal direction with the use of thrusters, full autonomous in normal conditions. These thruster forces can be neglected when the grab has ground contact, due to the weight of the grab and forces of the closing clamshells. A deep sea mining process as shown in Figure 1 has not yet been performed. A comparable operation with a suspended grab has been applied for a dredging operation at a water depth of about 120m (Es 2004 [10]).

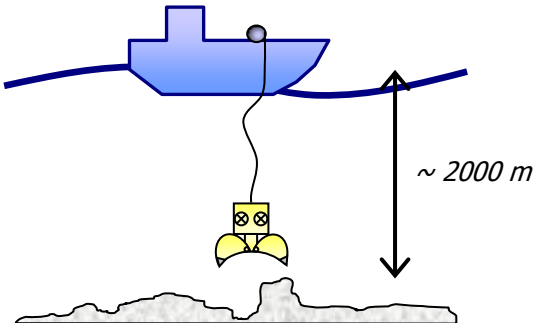

Figure 1: Situation Overview of a deep sea mining process

In Figure 2 are the degrees of freedom shown of a suspended grab with hydraulic actuated clamshells, which can move vertical by changing the length of the suspended cable and horizontal by actuating the thrusters on the grab. The heading of the grab can also be controlled by actuating the thrusters, however the heeling and pitch angle cannot be controlled, but are stable when free hanging on the hoisting cable due to the low center of gravity in comparison with the suspension point. The clamshell angles are both actuated with hydraulic cylinders and are individually controlled. Almost all degrees of freedom are in local coordinates, except for the vertical position and the heeling and pitch angle due to the hoisting cable force.

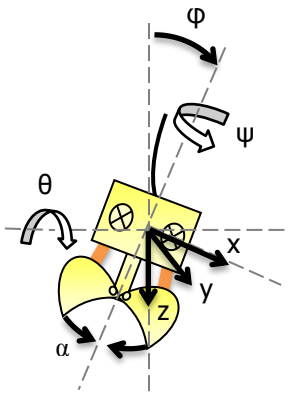

Figure 2: Degrees of freedom of a suspended grab, shown in coordinates of control

Degrees of freedom:

- Heeling angle φ
- Pitch angle θ
- Heading angle ψ
- Sideways translation x
- Forward translation y
- Vertical translation z
- Clamshell angle α

1.1.2 Controlling a Grab

Controlling a suspended grab during teleoperation is done with the use of joysticks; controlling both the grabbing force from the clamshells, as the cable hoisting force from the winch as shown in Figure 3 a) and b). The winch drum is located on the deck of the ship and has a large delay for controlling the cable hoisting force due to the size of the drum and length of the cable.

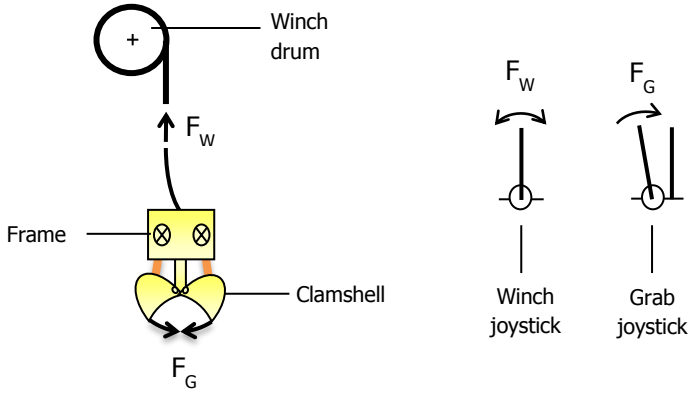

Figure 3: a) Schematic view of control parameters of actuators on slave. b) Schematic view of control parameters of joysticks on master

Controlling the cable force is used to lower or uplift the grab from the seabed and to prevent the grab to tumble over during ground contact. The closing force of both clamshells is controlled with the use of one joystick, because the grabbing force can only occur between both clamshells. Both joysticks for controlling the cable and grab forces will eventually be combined in a single joystick with two functions, rotating and grasping. Separation of both joysticks is chosen for this thesis to simplify the mechanical setup. The overview of the control system of the human operating the grab by tele-operation is shown in Figure 4. The red arrows indicate the feedback of the joystick on the human hand, force, velocity and position of the joystick angle. The blue lines from the controller indicate the current on the electric motors, actuating haptic feedback to the human. The green dotted line represents the visualisation feedback to the human operator, displaying the remotely controlled operation. The environment acts on the grab behaviour and back, the controller has different settings, from the control panel for different conditions. The human operator gets instructions to control the process.

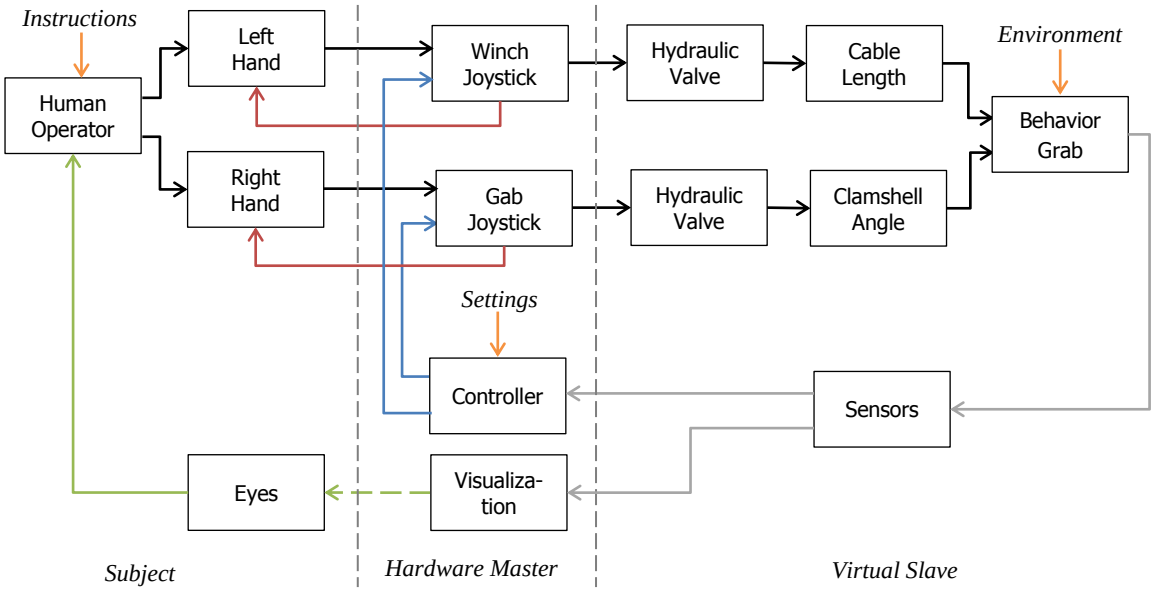

Figure 4: System control overview for tele-operating a remotely controlled grab. Red lines indicate feedback on human hand, blue lines current on electric motors, green lines visual feedback and orange lines system inputs.

1.1.3 Principle Hydraulic Actuators

A deep sea mining excavation process with a suspended grab consists of two main components, the winch drum and clamshells as described in paragraph 1.1.1 and shown in Figure 3 a). These two components control the two main parameters, cable force and cutting force, with hydraulic actuators. The winch drum is actuated with hydraulic motors and the clamshells with hydraulic cylinders. Both hydraulic actuators are based on the same principle of compressed hydraulic fluid forcing the actuator to move with a controlled velocity and force. The amount of force and velocity of the actuator is controlled with a valve, restricting the incoming flow as shown in Figure 5.

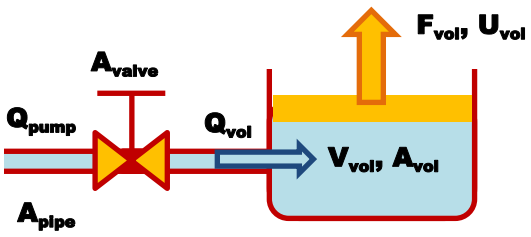

Figure 5: Schematic view of principle of hydraulic volume with controlled inflow

The flow through the valve as shown in Figure 5 is defined as a ratio of area as show in Eq. 3.

$$Q_{vol} = A_{valve} \frac{Q_{pump}}{A_{pipe}} \quad \text{Eq. 3}$$

The velocity of the volume level is defined as flow Q over area A as shown in Eq. 2.

$$U_{vol} = \frac{A_{valve}\, Q_{pump}}{A_{vol}\, A_{pipe}} \quad \text{Eq. 2}$$

The calculated velocity in Eq. 2 is based on a non-loading condition of the hydraulic actuator. A constant loading condition is given in Figure 6, describing the principle of compression of a fluid for changing volume at applied pressure.

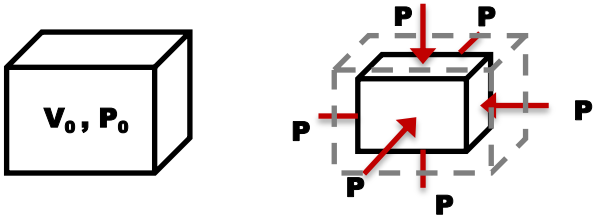

Figure 6: Principle of uniform compressed hydraulic volume.

Elasticity of a fluid as shown in Figure 6 is expressed with the bulk modulus, the reciprocal of compressibility, relating specific volume and differential pressure (George and Barber 2007 [11]). The definition of bulk modulus is given in Eq. 1 (Totten 1999 [36]).

$$B = -\frac{\Delta P}{\Delta V / V_0} \quad \text{Eq. 1}$$

Reversing Eq. 1 gives an equation for the pressure of the fluid, shown in Eq. 5. The volume of the fluid itself is defined as the integral of the inflow of the fluid.

$$P = B_{fluid} \frac{V_{fluid} - V_{vol}}{V_{vol}} - P_0\,, \quad V_{fluid} = \int Q_{cyl}\, dt + V_0 \quad \text{Eq. 5}$$

The force of the hydraulic volume as shown in Figure 5 is defined as pressure over area, as shown in Eq. 4.

$$F_{vol} = \frac{B_{fluid}\, A_{valve} \left(V_{fluid} - V_{vol}\right) A_{vol}}{V_{vol}\, A_{pipe}} \quad \text{Eq. 4}$$

Sub conclusion

Eq. 2 and Eq. 4 give the definitions of velocity and force related to the control valve area as shown in Figure 5. The combination of both equations therefore gives for controlling the inflow a transition of controlling the velocity to rate of loading, when the hydraulic actuator changes in loading condition. This results in a velocity controlled task for the operator when no contact is made and converts into a force controlled task during contact. This means a velocity task for controlling the winch drum when the grab is free hanging and controlling the cable force when the grab has contact with the seabed. For controlling the clamshells, the velocity is directly controlled after breaking rock material and force controlled before the breaking point of rock material.

1.1.4 Task Decomposition

A deep sea mining process consists of multiple tasks to be conducted, based on various fields of expertise. Evidently the entire process starts with exploration of the seafloor determining the location of the minerals.

After exploration an operating area is chosen and a ship is positioned for optimal production. Subsequently the following process steps are required for excavation of mineral deposits using a suspended hydraulic grab.

- Lower grab from ship to deep water.
- Planning of optimal excavation locations.
- Horizontal position grab on excavation location, while rejecting disturbances.
- Lower grab for contact with seafloor, using maximal impact for initial rock breaking.
- Closing the clamshells and controlling the grab force during cutting of the material and stabilizing the grab using cable forces.
- Uplift the grab from the seafloor.
- Translate the grab to a central collection point on the seafloor.
- Discharge the rock material at the collection point.
- Vertical transport of the material to the ship.
- Process the material on deck of the ship.
- Transport the material using bulk carriers.

In the enclosed blue area are the tasks listed that are the focus of this research, controlled by tele-operation. These tele-operations could be improved by offering natural force feedback to inform the operator of the environmental forces and haptic shared control with attractive guiding forces to assist the operator. In Figure 3 b) are the two joysticks shown to control this teleoperation, a grab joystick for closing the clamshells and a winch joystick for controlling the cable forces. The natural feedback forces to be offered on the grabbing joystick can be based on the cutting forces from the hydraulic cylinders, for the winch joystick the cable forces of the winch drum can be used. Guiding forces on the winch joystick can be used to assist the operator for controlling the correct cable force. The cable force has to be high enough for tension in cable to avoid tumbling over. The cable force also has to be not too high to remain vertical forces of from the weight of the grab on seabed for cutting the rock material. This required vertical force reduces when the clamshells are more closed also the required cable force for stable position of the grab has to increase when closing the grab. Figure 7 shows the change in degrees of freedom during transition of free hanging and ground contact. During free hanging the thrusters can translate the grab in the horizontal plane and change the heading angle. However during ground contact the thuster forces are limited compared to the contact and cutting forces, approximately 5% as calculated in part 1 of the thesis. Therefore during contact the cable and cutting forces dominate the behaviour of the grab and when incorrect controlled they can cause a large heeling angle of the grab, possibly damaging the machine. When the ground reaction forces are uneven, the cable force actuated with the winch has to stabilize the grab. However the cable forces have to be as low as possible to increase the vertical component of the cutting forces to break the rock material, without causing slack in the cable resulting in late response of the cable forces. Guiding forces on the control inputs could therefore help the operator to correctly control the winch. When the clamshells are almost closed the cable forces have to be increased to prevent instability of the grab, which can be informed with guiding forces to the operator as well. Natural force feedback gives the operator information of the acting forces and improves the awareness of the operator of the current situation, hence improving the correct control.

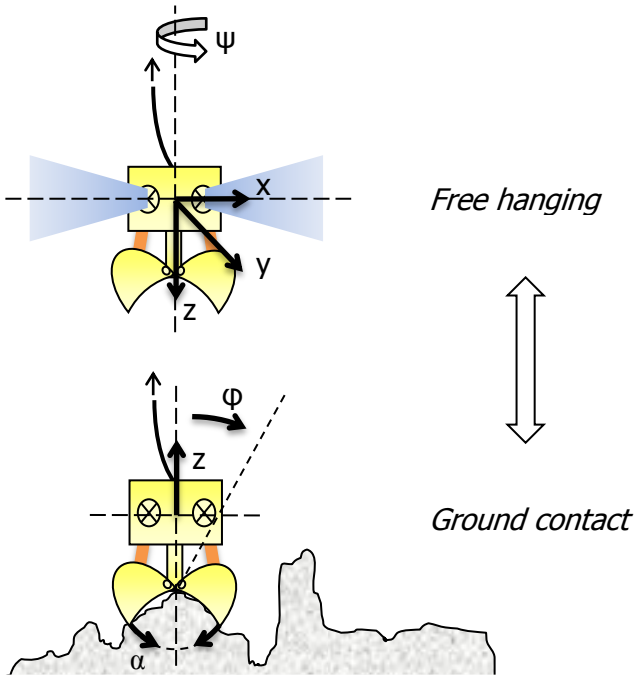

Figure 7: Change of grab movement during contact transition

1.2 Tele-operation

A deep sea mining operation consists of a suspended grab hanging from a ship as shown in Figure 1. Rock is excavated from the seabed, by controlling the position and cutting force of the grab remotely from the ship, using teleoperation. Teleoperation is remotely sensing and manipulating a device through means of communication using artificial sensors and actuators (Sheridan 1989 [33]). A high level of tele-presence describes the operation when a tele-operator feels physical present at the remote location, using ideal communication of the environment (Sheridan 1989 [33]). Difficulties in creating a high level of tele-presence are time delays, accuracy and limiting sensory feedback mechanism. These time-delays and low accuracies can even cause instabilities in controlling a teleoperation (Hannaford 1989 [14], Niemeyer and Slotine 1991 [26], Sayers et al. 1998 [31]). A method for increasing the level of tele-presence is the use of augmented reality, the addition of a virtual environment displayed to the operator based on sensory information (Milgram et al. 1995 [24]). In Figure 8 is a master-slave system shown, where the operator's movements on the input device (master) are mimicked by the remote controlled device (slave), combined called tele-manipulator (Sheridan 1989 [33]).

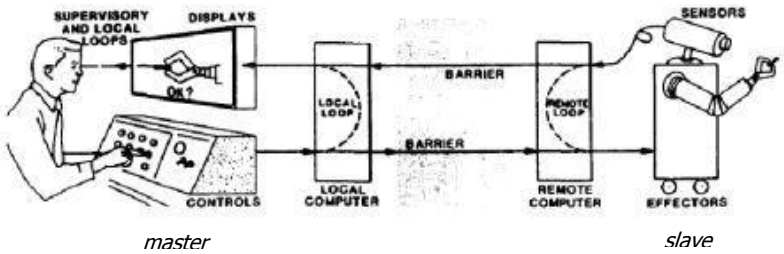

Figure 8: Schematic view of a teleoperation with visual feedback (adapted from Sheridan 1989 [33], pp. 2)

Teleoperation using only visual feedback would be applied for a deep sea mining process, controlling a suspended grab as shown in Figure 1. Haptic feedback could improve this teleoperation and therefore increase the level of telepresence. Two types of haptic feedback mechanisms to improve the human-machine interface are found in literature; natural force feedback, described in paragraph 1.2.1 and haptic shared control, described in paragraph 1.2.2.

1.2.1 Natural Force Feedback

Natural force feedback reflects forces acting on the slave part of a teleoperation to the operator, based on sensor information of the environment. Transparency in the teleoperation is the reflection of perceived inertia, damping and stiffness of the slave to the master as schematically shown in Figure 9 b) (Hannaford 1989 [13], Hannaford 1991 [15], Yokokohji 1992 [40], Abbot and Okamura 2003 [2]). The schematic representation as shown in Figure 9 b) resembles the experimental setup of Abbot and Okamura as shown in Figure 9 a), to determine the effect of different control architectures based on position and force feedback for applying forbidden regions in a teleoperation (Abbot and Okamura 2003 [2]).

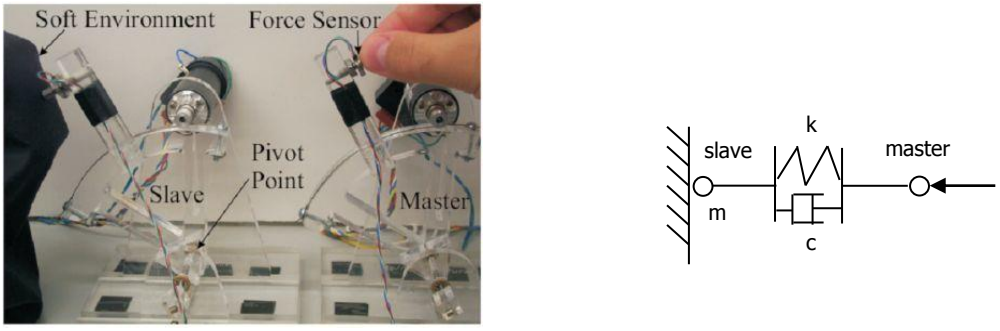

Figure 9: a) A 1 DoF Transparent Feedback Mechanism experiment for contact probing (adapted from Abbot and Okamura 2003 [2], pp. 2). b) Schematic representation of 1 DoF transparent feedback mechanism with artificial mechanical properties; mass m, stiffness k and damping c.

A transparent master-slave system as shown in Figure 9 a) consists of several dynamic properties, such as mass, stiffness and damping as shown in Figure 9 b) and displayed to the operator using force feedback. The dynamic properties are based on the dynamics of the object, master and slave device and the operator himself, as shown in Figure 10 (Yokokohji 1992 [40]).

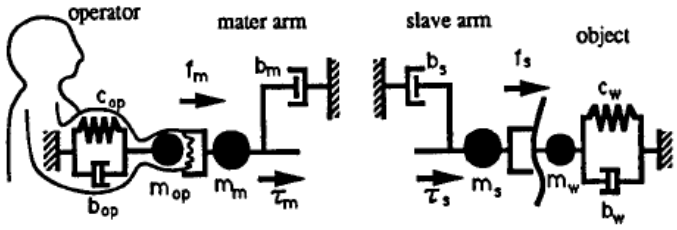

Figure 10: a) Schematic view of dynamics in transparent teleoperation of master and slave arms, operator and object (adapted from Yokokohji 1992 [40], pp. 850).

Scaling

In a deep sea mining process the forces acting on the slave part of the teleoperation, the hydraulic grab, cannot be directly reflected to the operator due to the size of these forces. These forces therefore need to be scaled down to the capability of a human operator. This can be done using a static geometric scaling factor or to add a dynamic part to this scaling factor as shown in Figure 11 (Kaneko et al. 1997 [20]). Scaling due to geometric differences is often needed, but scaling due to maximum capable force differences can also occur. The maximum occurring forces of a hydraulic grab is limited by the available hydraulic power of the

machine and can therefore be scaled down using the maximal occurring hydraulic pressure of the actuators for both winch and grab control as shown in Figure 3.

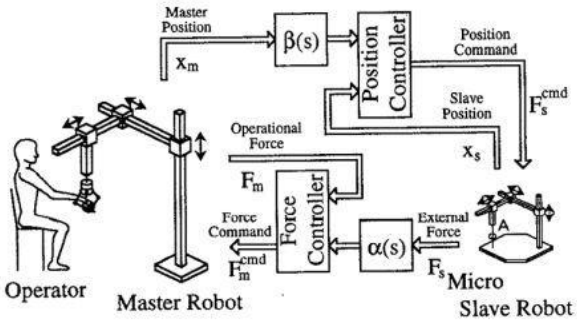

Figure 11: Transparent Feedback Application with impedance shaping scale factors (adapted from Kaneko et al. 1997 [20], pp. 71).

Control Architectures

Traditional teleoperation systems with natural force feedback consist of two channel system architectures, which can be position-position, position-force and force-force systems (Hannaford 1989 [13], Hannaford 1991 [15], Yokokohji 1992 [40], Abbot and Okamura 2003 [2]). Lawrence proposed a multivariable system architecture for achieving transparency and optimizing the results (Lawrence 1993 [21]). He introduces the use of four-channel data transmission between master and slave; velocities and forces in both directions as shown in Figure 12. Combined with this feedback mechanism he designed a tool for quantifying teleoperation system performance and stability under time delay. Where the tools for quantifying stability and performance relates to Niemeyer and Slotine of force reflecting systems operating under time delay (Niemeyer and Slotine 1991 [26]). Zhu and Salcudean used the four-channel data transmission structure to achieve transparency in their system when using rate and force control instead of position control (Zhu and Salcudean 1995 [41]).

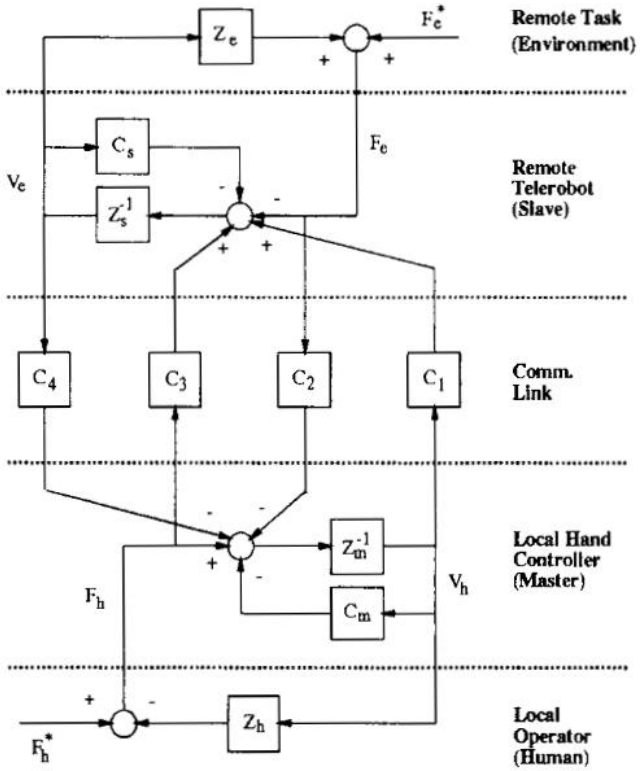

Figure 12: Transparent feedback control algorithm using a four channel structure, depicted with gain C1-4 of forces and velocities both ways (adapted from Lawrence 1993 [21], pp. 626).

Offering natural force feedback has shown improvements of the situation awareness of the tele-operator (Endsley 1995 [9]). Considerable amount of research has been done to improve the quality of natural force feedback, but perfect transparency has not been realized yet. Commercially available master-slave systems often employ non-optimized controllers, such as 2-channel force feedback, which inherently limits transparency. Still, even rough indications of contact forces can benefit tele-operation processes, although marginally (Wildenbeest et al. 2010 [39]).

Sub Conclusion

Offering natural force feedback to reflect slave forces on the master creates transparency in the system, increasing the operator's level of tele-presence. The reflected forces need scaling for a deep sea mining, due to the high operating forces. The forces reflected using a two way feedback structure would be sufficient and could improve the situation awareness, however is still limited and never completely transparent.

1.2.2 Haptic Shared Control

Natural force feedback as described in paragraph 1.2.1 reflects naturally occurring system forces to the operator, based on sensor information. The quality of this force feedback method is therefore as good as the sensor feedback with its time delays. Inaccurate sensor information and environmental uncertainties also prevent full automation for a deep sea mining process. The necessity for some form of manual control was already described by Tomovic due to limitations of full control in uncertain environments (Tomovic 1969 [35]). Not all events can be captured using a mathematical decision model in real-life situations with sensory and environmental inaccuracies. Unexpected events can occur, which cannot always be foreseen, or even sensor failure can occur. This will render autonomous control inapplicable, and will require the human operator to suddenly take over control, which is difficult when he is not used to control the operation manually (Endsley 1995 [9]). Shared control is therefore developed as a combination of manual control and

automation, a continuous shifting of authority as shown in Figure 13. The first found literature of shared control is by Hayati and Venkataraman, where a task-level sharing is applied (Hayati and Venkataraman 1989 [17]). The planning of the controlled path is shared with an autonomous controller and manual input from an operator.

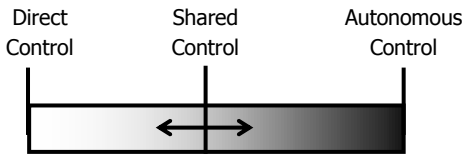

Figure 13: Schematic view of principle of haptic shared control, for continuous shift of authority.

Shared control is mainly applied in two ways, input-mixing shared control and haptic shared control. The most common and widely used manner is input-mixing, where the controller takes over the operators tasks in critical situations and disconnecting the controller inputs from the process. The disconnection of the control inputs creates difficulties for the operator to understand the process and the control actions. Haptic shared control on the other hand provides forces to the operator, when the operator diverts from the controllers optimal path for instance and keeping the connection of the control input to the process. The application of mixed inputs has been applied on a wide range of tele-operations (Hayati and Venkataraman 1989 [17]). However it does not seems the most promising solution for optimizing the human-machine interface because it is not keeping the human in the loop and simply takes over control, therefore greatly reducing the operator's situation awareness (Endsley 1995 [9]). The automatic controller is more detectible when applying a haptic shared control, this can be done using virtual fixtures or to apply artificial guiding forces to the operator.

Virtual Fixtures

Rosenberg, introducing Virtual Fixtures (VF) (Rosenberg 1992 [29]), has done one of the first steps in designing the sharing of control of an operator and automatic controller. The application of VF is a fairly simple concept for controlling a path with a master-slave combination. Where the optimal trajectory is calculated and certain boundaries are applied to guide the operator over the path as shown in Figure 14.

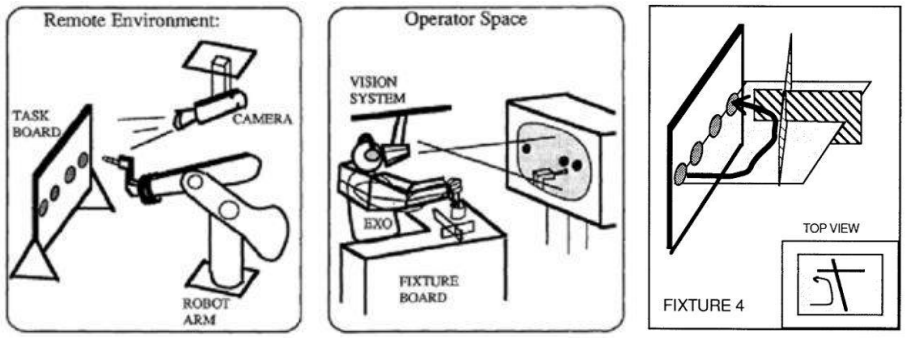

Figure 14: Principle of Virtual Fixtures for trajectory control (adapted from Rosenberg 1992 [29], pp. 15, 20).

The virtual fixtures presented by Rosenberg were virtual walls in space to guide the human operator, this was felt as a hard wall. Abbot and Okamura further looked into this hardness of the wall and presented it as Forbidden-Region Virtual Fixtures (FRVF). They experimented with hard and soft virtual fixtures to guide the operator (Abbot and Okamura 2003 [2]). They also experimented with virtual fixtures at the master or at the slave side of the device. They concluded that only a hard VF at the master side is giving poor results and that the best results came from a soft VF at both ends for their 1 DoF system as shown in Figure 9 a).

Artificial Guiding Forces

When applying a soft virtual fixture to the system, the operator is guided to stay in the correct zone of operation. With the use of a soft virtual fixture, the operator can even be guided to the most optimal path (Sayers and Paul 1994 [30], Abbot and Okamura 2003 [2], Bettini et al. 2004 [5]). A hard VF would make it impossible to deviate from that path and therefore almost leaving no control to the operator. A guiding force can therefore help the operator to stay on the path, but allows deviation in case of overruling by the operator. The guiding control can also be split up into an attractive or repulsive control as illustrated in Figure 15 (Prada and Payandeh 2009 [28]). The soft virtual fixtures are all repulsive forces, applying forces to the operator to stay out of certain region. But when the repulsive field is all around the optimum path and directs the operator down the path, an attractive force is applied. The attractive force is directing the operator over the path. When the operator does not hold the master device, the controller would even operate completely autonomous.

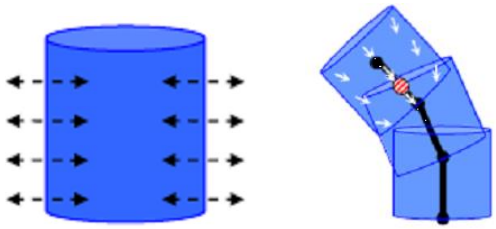

Figure 15: a) Principle of 2 DoF repulsive artificial guiding, (adapted from Prada and Payandeh 2009 [28], pp. 121). b) Principle of 2 DoF attractive artificial guiding (adapted from Prada and Payandeh 2009 [28], pp. 127).

Attractive guidance forces are mostly applied when offering haptic shared control with guidance on a tele-operating task (Boessenkool et al. 2011 [7], Mulder et al. [25]). This is proven to increase the performance of an operator when conduction free-air movements, however for contact or rotational tasks this did not show any improvements (Boessenkool et al. 2011 [7]). Also attractive guidance is usually applied in position controlled tasks rather than rate controlled. However the research of Abbink showed a rate or even acceleration controlled task with a similar guidance feedback for controlling the throttle of a car, which is focussed on the relative velocity between two vehicles and therefore a sort of rate controlled task (Abbink 2006 [1]).

Control Architectures

Haptic shared control is a continuous combination of manual control and automation as shown in Figure 13. Both the human operator and automation control the teleoperation by applying forces on the master input device. The human operator therefore directly notices the actions of the automation and is able to confirm its actions or disagree. This creates a continuous shifting of authority of controlling the teleoperation. Virtual fixtures creates a virtual contact comparable with natural force feedback, but can be disagreed by the human operator. Artificial guiding forces are applied continuous and therefore give a continuous feedback of the optimal path to the operator. The level of continuous feedback forces depend on the diversion of slave from the optimal path. When combining the level of control action into these feedback forces, a stiffness feedback is created (Hogan 1984 [19], Abbink et al. 2008 [2]). This is best described with an application in the automotive sector for throttle control of a vehicle (Abbink 2006 [1]), and to apply this for a rate controlled task of a deep sea mining process with hydraulic actuators as described in paragraph 1.1.3. Artificial guiding forces are applied on the gas pedal of the car for assisting the driver to keep a safe driving distance from the next vehicle in front and prevent collision. The level of force feedback is calculated from the time headway as shown in Figure 16 a). This feedback force can be applied purely depending on the time headway, or on a combination of the pedal depression creating a stiffness feedback as shown in Figure 16 b). The use of stiffness feedback rather than force feedback is useful for controlling a deep sea mining application with a joystick due to the bidirectional input device, which would be instable with direct force feedback.

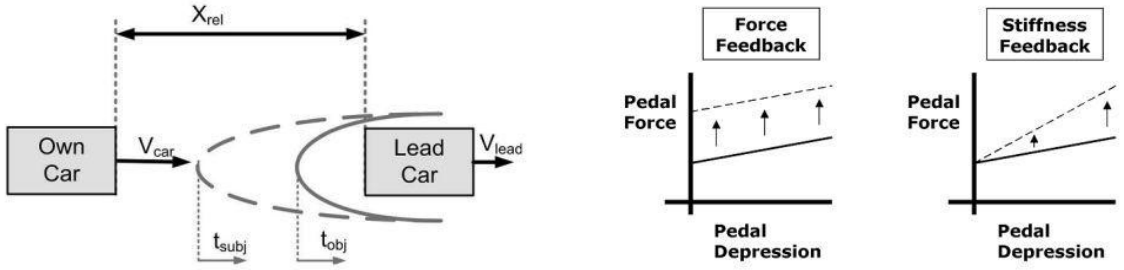

Figure 16: a) Car Following Application of Shared control (adapted from Abbink 2006 [1], pp. 19). b) Schematic representation of force and stiffness feedback mechanism (adapted from Abbink et al. 2008 [2], pp. 7).

The design of the guiding forces to be offered to the operator using stiffness feedback can be best shown with the example of throttle control of Abbink (Abbink et al. 2008 [2]). A Driver Support System (DSS) is developed as automatic controller to measure time headways and apply forces on the gas pedal. The forces on the gas pedal are detected by the human operator, which decides to confirm or disagree with these actions based on visual feedback of the situation as shown in Figure 17.

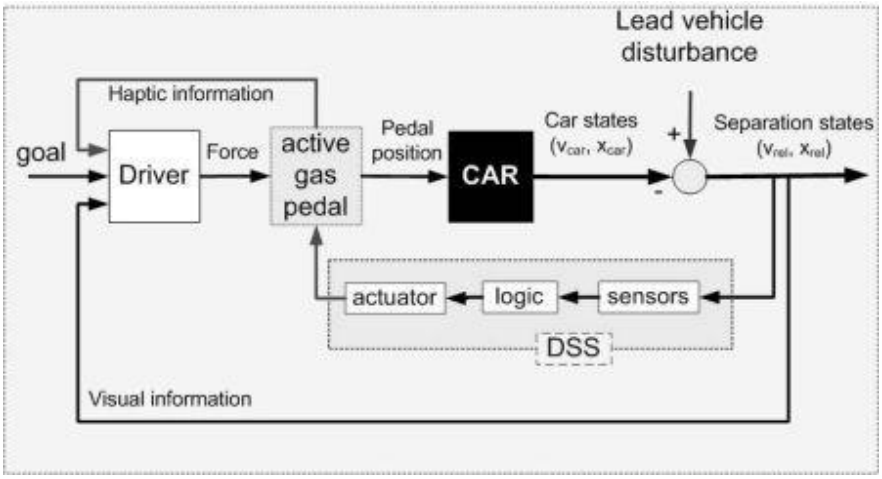

Figure 17: Shared Control Algorithm for car following with guiding haptic force feedback (adapted from Abbink 2006 [1], pp. 7)

Sub Conclusion

Virtual fixtures in a deep sea mining process could prevent the operator to operate out of capabilities of the machine and prevent incorrect control actions of the operator. Attractive artificial guiding forces could assist the human operator in continuous operation to increase the performance of the operation and reduce control effort by guiding the operator to the optimal control. Attractive artificial guiding is up to now only applied for position tasks, when the controller can determine an optimal path. Therefore applying attractive artificial guiding forces for a rate and force task of a deep sea mining excavation operation needs to be investigated. For the cable forces controlled with the winch drum as shown in Figure 3 a), the application of haptic shared control could improve the teleoperation of a deep sea mining operation by guiding the optimal cable force to apply.

1.3 Grasping with Tele-operation

One of the main processes during a deep sea mining operation is cutting rock material from the seabed. This will be done using a large-scale hydraulic actuated suspended grab to cut the rock material as shown in

Figure 1. The rock material will be cut by closing both clamshells of the grab using a single joystick with a grasping motion as shown in Figure 3 b). Grasping with teleoperation can also be improved using haptic feedback to improve the level of tele-presence as described in paragraph 1.2. Most of the research for haptic feedback is applied on tele-operations controlled with arm movements, which differs for a grasping teleoperation fully controlled with hand movements and forces. Several research of grasping with natural force feedback is described in paragraph 1.3.1 and the use of haptic shared control for grasping in paragraph 1.3.2.

1.3.1 Grasping with Natural Force Feedback

The use of natural force feedback is besides contact forces also applied on grasping forces, to increase the transparency of the system during a grasping task. Transparency in a grasping teleoperation can be expressed with the teleoperation stiffness and damping (Christiansson et al. 2008 [8]). Research has been done to determine the effect of stiffness and damping for performance of discriminating objects during teleoperation as shown in Figure 18 a) (Christiansson et al. 2008 [8]). No improvements of performance for object discriminating was found for improving quality of feedback, when tele-operator stiffness higher than environmental stiffness. Natural force feedback is as well applied for manipulation of objects using dexterous teleoperation, as shown in Figure 18 b). Using an instrument glove witch an exoskeleton attached, the operator could feel the applied forces of the slave robot to hold and manipulate objects. Experimental results did not show an improvement in task performance for the addition of natural force feedback due to imperfect force transparency (Turner et al. 2000 [38]).

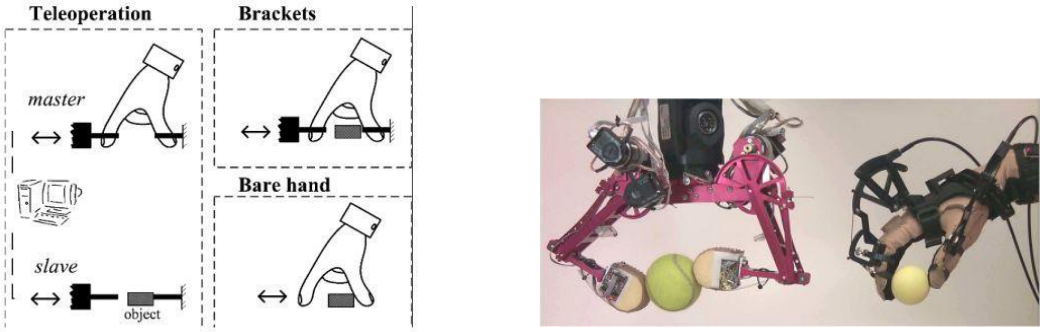

Figure 18: a) Discriminating object with teleoperation (adapted from Christiansson 2008 [8], pp. 1253). b) Grasping of objects using teleoperation (adapted from Turner et al. 2000 [38], pp. 1).

Sub Conclusion

The use of natural force feedback to increase situation awareness for grasping teleoperation did not show an increase in task performance. However some indication was found of improving learning curve and reduction of control errors compared to manual control. Natural force feedback applied on the grasping teleoperation of a deep sea mining process controlling the cutting force could therefore improve the situation awareness of the process and reduce control errors in controlling the cable force.

1.3.2 Grasping with Haptic Shared Control

Shared control is also applied for manipulation of objects using dexterous teleoperation as shown in Figure 19 a). The automated controller assisted the operator to hold the objects with the correct grasping force using input-mixing shared control (Griffin et al. 2003 [12]). The automated controller intervened when incorrect grasping forces were applied, combined with visual and auditory feedback. Due to intervention of the applied grasping force, the target window for desired forces could be enlarged as shown in Figure 19 b). This resulted in improved task performance using shared control for a grasping task in combination with visual and auditory feedback.

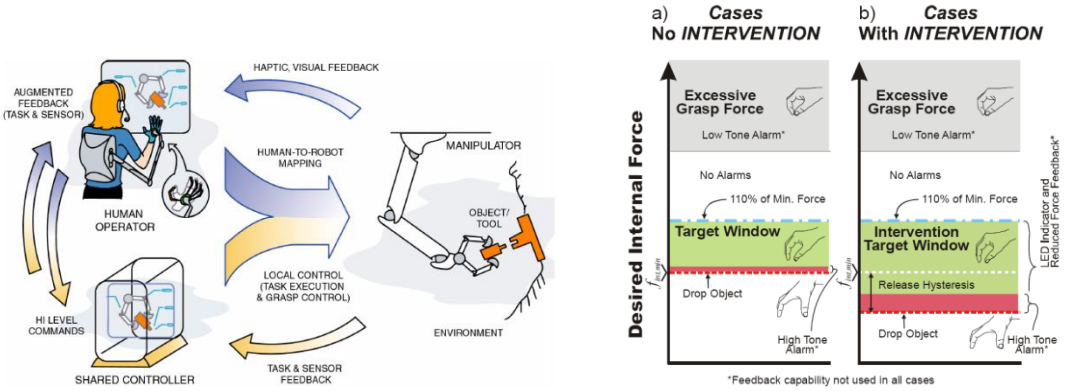

Figure 19: a) Schematic representation of Grasping Objects with Shared Control (adapted from Griffin et al. 2003 [12], pp. 1). b) Methods of feedback to the operator for grasping with shared control (adapted from Griffin et al. 2003 [12], pp. 3).

Sub Conclusion

Besides input-mixing shared control, no literature was found describing haptic shared control, guiding or restricting the operator during a grasping task. However shared control did show improvements in grasping task performance. Haptic shared control could alert the operator when cutting forces are too low or high and guide the operator to apply the correct forces. This can be applied when clamshells are closed and no high cutting force is necessary.

1.4 Problem Statement and Goal

Realizing a deep sea mining process is not been done so far due to technical difficulties and uncertainties of economic feasibility. However at this moment a number of remaining technical difficulties for this process such as the level of rock cutting forces and vertical lift mechanism of the material are being researched. This thesis focusses on improving the human-machine interface for controlling deep sea mining excavation process by applying haptic feedback to the operator. Controlling a deep sea mining excavation process by tele-operation using only a standard human-machine interface with visual feedback is difficult for the operator. The operator's situation awareness is limited by the feedback of the process, therefore making a tele-operation of a large machine on great depths a complex procedure. Consequently this reduces the process efficiency and can even cause control errors in critical processes. The aim of this research is to improve the human-machine interface by offering haptic feedback to the operator, by offering 'natural force feedback' and by offering 'haptic shared control'. Both have never been designed for deep sea tele-operated manipulation and not applied for a rate and force controlled task.

1.5 Hypotheses

It is hypothesised that natural force feedback will not affect performance, but will increase situation awareness for a teleoperation of deep sea mining using a grab. This will result in reduced control errors that would otherwise cause incorrect behaviour of the grab and increased response time in critical processes. It is also hypothesised that haptic shared control will improve the teleoperation performance and reduce the control effort of the teleoperation. This will result in increased production results for rock excavation and reduced control angles during deep sea mining processes in normal conditions. The summary of the

hypotheses for the effect of both haptic feedback mechanisms on the performance is given in Table 1, control effort in Table 2 and situation awareness in Table 3.

Conditions	No NFF	NFF
No SC	0	+
SC	+	++

Table 1: Hypotheses of increase of performance results for all conditions

Conditions	No NFF	NFF
No SC	0	0
SC	+	+

Table 2: Hypotheses of reduction of control effort results for all conditions

Conditions	No NFF	NFF
No SC	0	+
SC	0	+

Table 3: Hypotheses of increase of situation awareness results for all conditions

1.6 Approach

The human-machine interface can be improved by applying haptic feedback, thereby it will increase the performance and situation awareness of the operator. Two haptic feedback mechanisms as described in paragraph 1.2 are stated in the hypotheses to improve the teleoperation. The hypotheses are tested with experiments to measure the improvements of each feedback mechanism for performance, effort and responses in critical situations. The experimental method is given in chapter 2, describing two types of tasks that were conducted by the subjects during the experiments at different conditions. Chapter 3 describes the design of the mechanical and software parts of the experimental setup. The results of the experiments are shown in chapter 4, which are further discussed in chapter 5. The conclusions of all hypotheses based on the experimental results are given in chapter 6. Chapter 7 gives further recommendations regarding the conducted experiments and validations of the stated hypotheses.

2 EXPERIMENT METHOD

Excavating rock material during a deep sea mining process using a suspended grab as shown in Figure 1 in paragraph 1.1.1 is a difficult procedure. Full automation is not feasable due to environmental uncertainties and sensor limitations. Controlling the process manual by teleoperation could be improved by using haptic feedback. Two haptic feedback mechanisms to improve the human-machine interface were found in literature and described in paragraph 1.2; natural force feedback and haptic shared control. Paragraph 1.1.1 described the deep sea mining process with a suspended grab and the control parameters as shown in Figure 3. An experimental setup is developed to validate the hypotheses as described in paragraph 1.5 for improvements of haptic feedback mechanisms for a deep sea mining process. The experiment consists of a human operator conducting a virtual deep sea mining task using two haptic joysticks and a display as shown in Figure 20 a) and b).

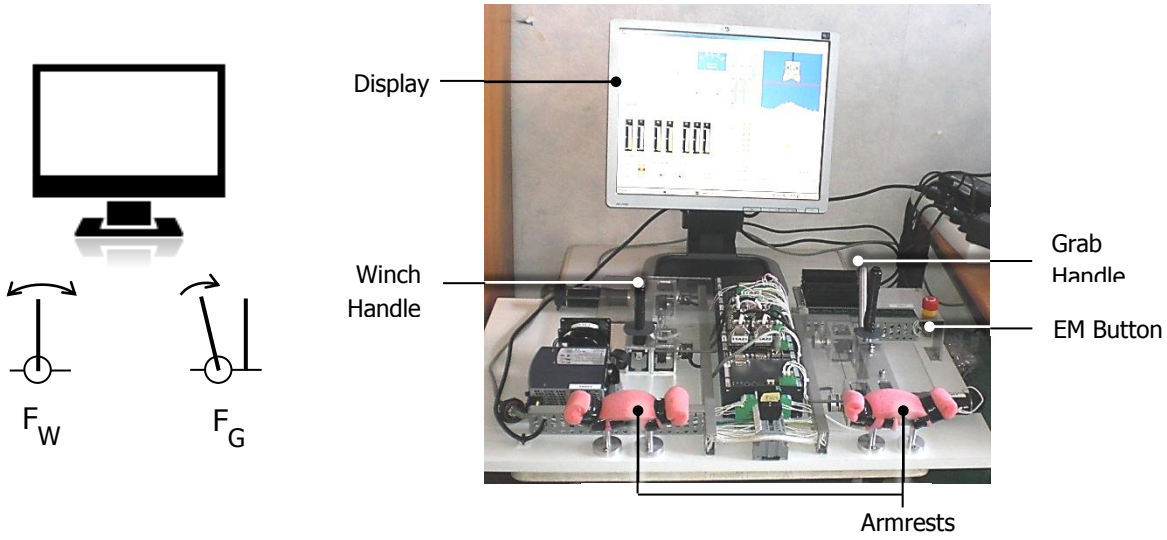

Figure 20: a) Schematic view of experimental setup with a display and two joystick handles. b) Overview of experimental setup with two joysticks and display.

A description of the process of the experiment is given in paragraph 2.1, describing the experimental setup and task to be conducted by the subjects. In paragraph 2.2 is a description of the experiment given, for conditions and measured variables.

2.1 Process Description

An experiment was conducted to validate the hypotheses of improvements of haptic feedback mechanisms for a deep sea mining process. The participating subjects are described in paragraph 2.1.1. A general description of the used experimental setup is given in paragraph 2.1.2, which is described in more detail in chapter 3. A description of the task is given in paragraph 2.1.3.

2.1.1 Subjects

Ten subjects in the range of 24 to 27 participated in the experiment, nine male and one female. None of the subjects had previous experience with teleoperation systems besides some gaming experience. All subjects were right handed and participated voluntarily without financial compensation for their time and effort. Only a small suiting prize was promised beforehand and given to the top three of best performing subjects, to increase the competitive behaviour for optimal concentration. Before conduction the experiment each subject

was given a written instruction that explained the experiment and setup to be controlled. After a short demonstration of the setup, each subject had at least ten practice trials, more if requested and included all conditions. A brief study was performed to determine the learning curve of the subjects for controlling this experimental setup and no improvements were found beyond just a few trials.

2.1.2 Experimental Setup

The experimental setup for controlling a deep sea mining process and control variables as shown in Figure 3, consist of two joysticks and a display as shown in Figure 20 a). The setup consists of an electro-mechanical master to be used as input device for the human operator to control the virtual slave robot. The master device consists of two force feedback joysticks and armrests as shown in Figure 20 b). Each joystick is actuated with an electronic planetary-geared motor, connected with cables and spring to create series-elastic actuation. Using two incremental angular encoders for each joystick, the position and force on the joystick can be measured. The joystick for controlling the grab force is a one directional joystick to control the closing force, combined with a button on top of the joystick the clamshells can be opened. On both joysticks were hall-sensors attached to detect contact of the operator, wearing magnets attached to the hand to prevent uncontrolled movement of the grab. The behaviour of the virtual slave robot is calculated with a mathematical model describing the kinetics of the machine and forces of the environment on the machine. A real-time controller applies feedback forces on the master device based on parameters gained from the virtual model, depending on the experimental conditions. The real-time controller runs on an industrial computer dedicated to real-time computing, connected to the sensors and actuators of the master device. The display in front of the operator shows visual information about the deep sea mining process gained from the virtual model. This visual feedback is shown to the operator in all experimental conditions. The visual feedback contains besides information of the behaviour of the grab also several control parameters, such as optimal cable force and predictions of ground contact and closed clamshells. Both the virtual model and the visualization run on two separate computers with a Windows XP operating system.

2.1.3 Task description

Each subject has to operate the system as fast as possible, when operating safely. This is stimulated by recording real-time the production of the task and previous tasks, displayed to the operator. A penalty of 300 seconds is given for a task when the subject makes an error during execution of the task. These errors can consist of a high heeling angle of the grab or a late response during mechanical failure. These penalties were applied to increase the attention level of the subject and add a competitive factor to the experiment, where the best results were awarded with a small prize. These time penalties were not taken into account for further analysis besides the number of errors made. An overview of the situation of excavating rock using a suspended grab is shown in Figure 21.

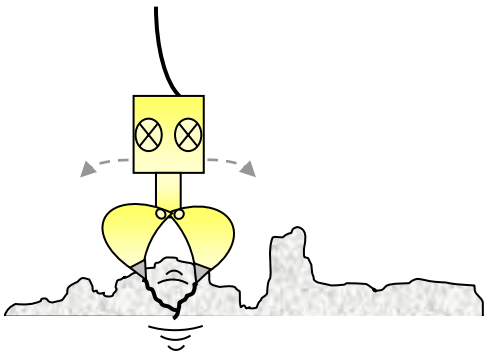

Figure 21: Situation overview of grab excavating rock on seafloor.

The excavation procedure using a suspended grab is shown in Figure 21, consisting of multiple stages.

In Figure 3 are the main control parameters shown to operate the deep sea mining process, also shown in Figure 20. The different stages for operating a deep sea mining excavation process with a grab mainly consists of the vertical transport and cutting process, as listed in Table 4 with the estimated task completion time.

Description	Estimated task time
Setting down the empty grab on the seabed	5
Starting the grabbing process	1
Controlling the grabbing process	30
Stopping the cutting process	1
Uplifting the grab with a full grab	5

Table 4: Task description of the conducted experiment for a grab with estimated task completion times

For each condition the subject had to execute six tasks, in random order for each condition. For each subject the executed tasks were randomized identical for each condition, only the order of conditions was changed for each subject. The six tasks to be executed per condition consist of three performance tasks to complete and three catch trials as listed in Table 5. The three performance trials are conducted for each experimental condition in normal situations and normal ground forces. The first catch trial is to see how the subject reacts under difficult situations, to see if the experimental conditions improve or confusing the operator during difficult situations. The difficult situation mainly consist of highly fluctuating ground forces due to small chip fractures, causing the grab not to penetrate the soil and merely scraping the surface. During the second catch trial the ground forces are exceeding the grab's capabilities, causing an incomplete cutting process. This task is added to increase the attention level of the subject and not expecting a full completion, but measuring response of the operator. The last catch trial consists of normal ground forces, but a mechanical failure after varying times and is used to measure the reaction times to this failure. This mechanical failure is only shown using visual feedback, indicating the level of attention of the operator and mental load of the process. All these six tasks are randomized for each condition in the same order for each subject.

Task	Category	Description
1-3	Performance	Normal conditions
4	Catch trial	Critical situation due to difficult soil, causing rotation of grab
5	Catch trial	Hard soil overall, unable to complete tha task and causing rotation
6	Catch trial	Reaction time of mechanical failure of pressure or temperature

Table 5: Different types of task description during experiment

The presented data in the results is reordered, in the order of 1-6 as described in Table 5. The shown ground pattern, displayed to the operator was also randomized. The ground pattern had no influence on the behaviour of the grab and was solely meant to mask the different tasks, so there was no recognition of the events.

2.2 Experiment Description

The experiment is conducted with the experimental setup as shown in Figure 20 to validate the hypotheses for improving the human-machine interface for a deep sea mining process. The different experimental conditions used during this experiment are described in paragraph 2.2.1 and the measured variables in paragraph 2.2.2.

2.2.1 Experimental Conditions

The experiment was developed to validate the hypotheses as stated in paragraph 1.5. Two methods for haptic feedback are described for improving the human-machine interface of a deep sea mining teleoperation; natural force feedback and haptic shared control. Both methods are applied in four different combinations for experimental conditions as listed in Table 6.

Condition	Description	Abbreviation
E.C. 0	Direct Control (baseline)	DC
E.C. 1	Haptic Shared Control	DC-SC
E.C. 2	Natural Force Feedback	FF
E.C. 3	Both Feedback Mechanisms	FF-SC

Table 6: Experimental Conditions

The baseline condition represents the current control application as applied in comparable situations of controlling a suspended grab. Visual feedback is applied during all four conditions, also showing the feedback parameters used for haptic feedback as described in paragraph 2.1.2 and described in detail in paragraph 3.3.2. The design of the haptic feedback mechanisms is based on stiffness feedback, adapted from Abbink which again was based on the impedance control of Hogan (Hogan 1984 [19], Abbink et al. 2008 [2]). The magnitude of the feedback force F for stiffness feedback depends on the angle of the joystick θ, therefore at increasing joystick angle an increasing feedback force is applied as shown in Figure 22 a). The total feedback force F_{max} determines the stiffness of the feedback and is adjusted depending on the environmental forces acting on the grab. The F_{max} is determined using sensor feedback of the hydraulic actuators of their operating pressure, causing the actuation force. Therefore the natural force feedback of the grabbing joystick depends on the hydraulic pressure in the clamshell hydraulic cylinders and the winch joystick on the hydraulic pressure of the winch hydraulic motors pulling the hoisting cable. The haptic shared control feedback forces depend on a shifting of the equilibrium point dθ of the stiffness feedback as shown in Figure 22 b) based on the literature of Mulder for guiding a steering wheel (Mulder, Abbink and de Boer 2008 [25]). Furthermore virtual fixtures are applied as shared control method limiting the joystick angle when maximal velocity of the actuator is reached, reducing the control effort. The application of feedback mechanisms is described in more detail in paragraph 3.3.3.

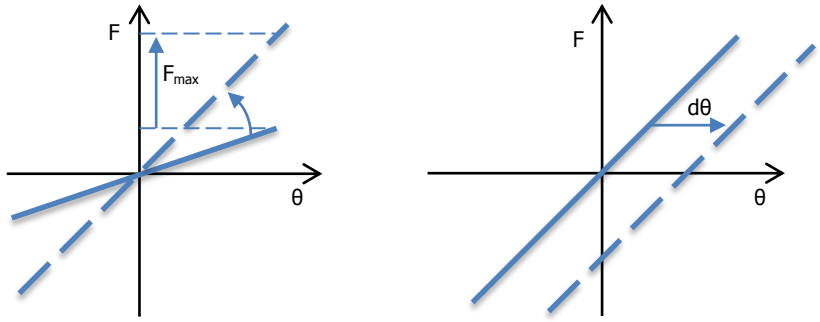

Figure 22: a) Stiffness feedback mechanism for haptic feedback on a joystick for natural force feedback. b) Shift of equilibrium point of joystick angle for haptic shared control using stiffness feedback.

The parameters used for haptic feedback are shown in Figure 23 for both joysticks with natural force feedback shown in blue and haptic shared control shown in red. The warning on the grab joystick uses a vibrating feedback force when applying an input force which is unnecessary after closing of the clamshells.

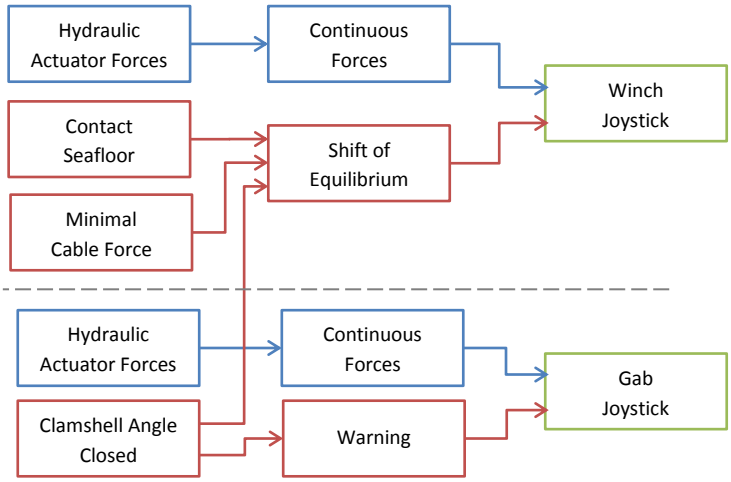

Figure 23: Decision model of the intelligent controller

2.2.2 Measured Variables

To analyse the effect of the applied haptic feedback mechanisms, a great amount of variables were measured of the human operator and virtual grab model. The variables were measured at different sample rates, depending on the rate of fluctuation of the variables to reduce the load of network communication. Several metrics were calculated based on the measured variables and categorised in four groups as listed in Table 7. The first three categories of the calculated metrics are measured objectively, except for the self-assessment category, which are subjective metrics. All metrics are used for analysing the three performance trials as listed in Table 5. For the first catch trial only the performance, system and control effort metrics are used. To analyse the second catch trial, only production time, frame angle and control effort is used. For the last catch trial none of the mentioned metrics are used and a new metric reaction time was used, only applicable for this tasks.

Performance	System	Control effort	Self-assessment
Time	Frame Angle	Summation Joystick Angle	Overall Workload
Volume	Cable Length Difference	Moving Joystick Angle	Overall Rating
Production	Force Setpoint Deviation	Applied Joystick Force	

Table 7: Evaluation metrics for evaluating experiment results in four categories.

To determine the subjective workload, the subject was asked to answer six brief questions at the end of every conducted task. These questions are based on Hart and Staveland's NASA Task Load Index (TLX) method to determine the subjective workload of an operation (Hart and Staveland 1988 [16]). The six questions are described in Table 8, which were asked for each six task, at all four conditions.

Title	Abbreviation	Description
Mental Demand	MD	How mentally demanding was the task?
Physical Demand	PD	How physically demanding was the task?
Temporal Demand	TD	How hurried or rushed was the pace of the task?
Performance	PE	How successful were you in accomplishing what you were asked to do?
Effort	EF	How hard did you have to work to accomplish your level of performance?
Frustration Level	FR	How insecure, discouraged, irritated, stressed, and annoyed were you?

Table 8: Questionnaire

Each question had to be answered by means of rating from one to twenty as shown in Figure 24. The total workload consists of a weighted average of all six questions for each task, with an equal weigh factor for all questions. The overall rating was asked in the end of the entire experiment for each subject, rating each experimental condition with the similar scale as shown in Figure 24.

Figure 24: Example question rating

2.2.3 Data Analysis and Statistics

The statistical data is displayed with the use of a box plot (McGill et al. 1978. The statistical data for each condition in the boxplots consist of the median (white circle), upper and lower quartile (blue/red tick line), extreme values (blue/red thin line), confidence interval of mean value (black triangles) and outliers (blue/red circles). Some of the data shows a wide confidence interval, exceeding the upper and lower quartile, due to the small sample size. The median of the baseline condition (grey dotted line) indicates the reference point of the data. First a one-way analysis of variance (ANOVA) is used for determining statistical significance in difference of means. A two-way ANOVA was chosen for correcting of variations between subjects, using (••) for $p \leq 0.01$, (•) for $p \leq 0.05$ and (-) for $p > 0.05$. The independent variables used for the statistical analysis are the experimental conditions as listed in Table 6 of the haptic feedback selection. The measured variables as listed in Table 7 of the evaluation metrics are the dependent variables, the outcome depending on the experimental conditions.

3 EXPERIMENTAL SETUP DESIGN

The experimental setup as shown in Figure 25 mainly consists of a display and two joysticks to operate a deep sea mining procedure, one joystick controlling the winch and one the grab. Both joysticks are one dimensional, controlling a velocity parameter of the process. The display shows a side view of the position of the grab and seafloor. Also position, velocity and force data of the controlled parameters and various additional parameters are shown to control the process.

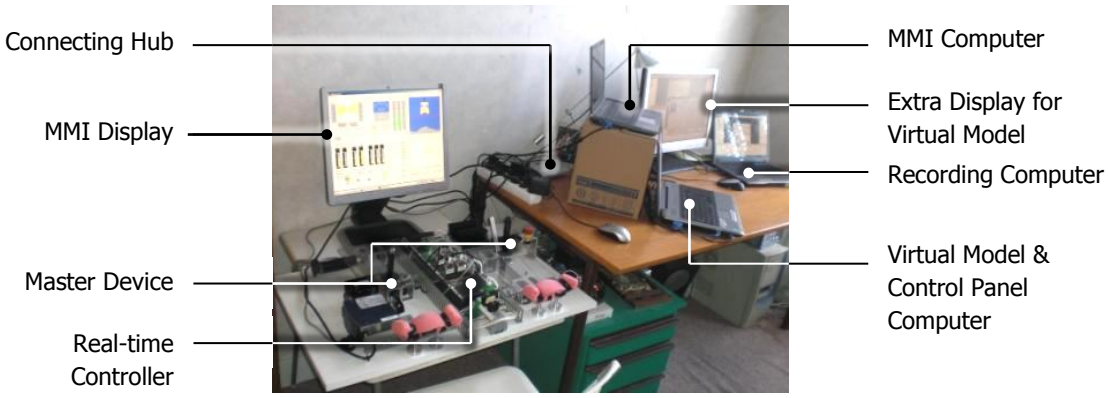

Figure 25: Complete overview of experimental setup with all connected hardware for controlling the setup.

The operator has to place both arms on the armrests and his hands around the sticks to control the process. The electronics for applying force feedback on the joysticks is placed on the same base in front of the operator, combined with a real-time controller placed in between the joysticks. The mechanical design is further described in more detail in paragraph 3.1. An overview and list of used mechanical and electrical components is given in paragraph 3.2. A detailed overview of the software structure, design of the visual interface, real-time controller and the mathematical model of virtual slave robot is given in paragraph 3.3.

3.1 Mechanical Design

The mechanical part of the experimental setup is designed to apply a constant high level of force on a joystick instead of vibrations as used in commercial available joysticks. Also an adjusted design was needed to create a grasping motion for controlling the cutting force of the grab, for eventually combining both joysticks. The mechanical principle of both joysticks consists of two pulleys connected with cables and springs as shown in Figure 26 a). The joystick handle is connected to one pulley and an incremental encoder, measuring the angular position as shown in Figure 26 b). An electrical geared motor is connected to the other pulley and an encoder. The relative measured distance of both angles represents the elongation of both springs, which have pretension to prevent slack in cables. This elongation is used in combination with the calibrated stiffness of the spring, to measure the force on the joystick handles.

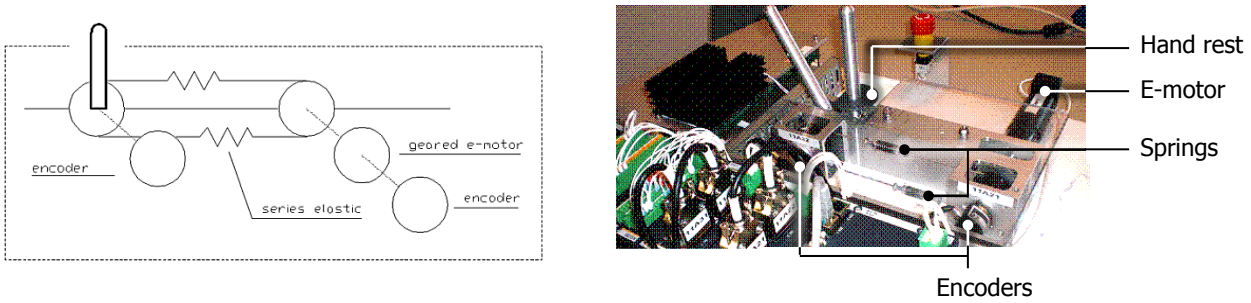

Figure 26: a) Schematic view of mechanical principle for a single joystick. b) View of experimental setup for the grabbing joystick.

Both pulleys are connected on steel axes, mounted with bearings in aluminium tubing for ensuring alignment of both axes. Two aluminium frames connect the two encoders on both axes, mounted with springs for alignment of the fragile incremental encoders. The joystick for controlling the winch drum is shown in Figure 27 a) and the clamshells is controlled with the joystick design as shown in Figure 27 b). Both joysticks are almost identical in design as shown in the figure. The main difference is the static pole attached on the base frame for the grabbing joystick as shown in Figure 27 b). The winch joystick has a slightly larger stroke, allowing bidirectional control.

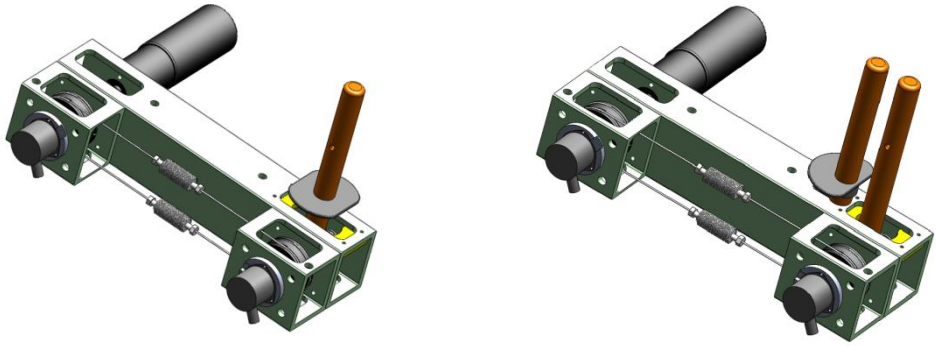

Figure 27: a) View of mechanical design of joystick handle for controlling the winch drum. b) Mechanical design of the grasping joystick for controlling the movement of the clamshells.

Both bases contain some drilled mounting holes for assembly purposes and are mounted on a base plate for alignment of the joysticks and armrest to operate the controls. The electronics for controlling the electrical motors and sensors also are mounted on this base plate as shown in Figure 28 a) and b), including the real-time controller in the middle.

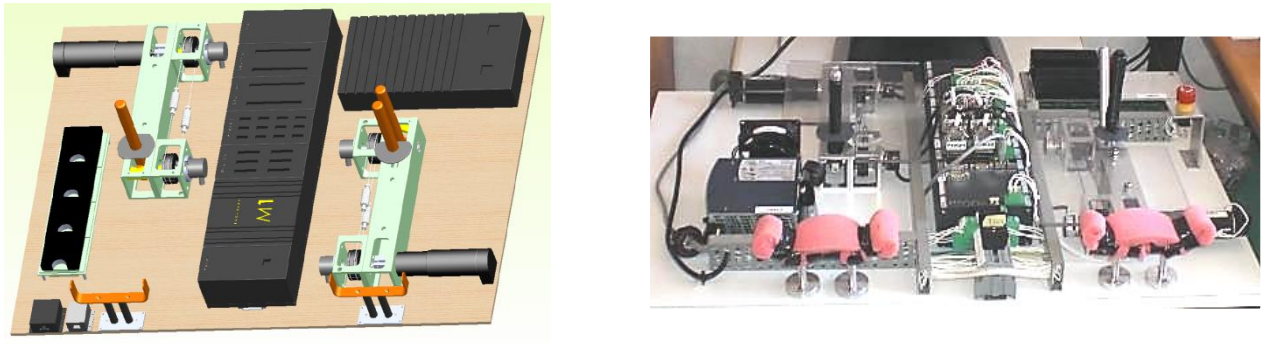

Figure 28: a) Design drawing of mechanical setup. b) View of master device of experimental setup.

3.2 Components

Most of the applied components in the experimental setup are mainly supplied on loan base for cost reduction. Reduction of design time was hereby also achieved because of pre-designs for the original applications of the components. The main mechanical components such as the joystick handles and base frames were specially designed and fabricated at Delft University of Technology (DUT), which also supplied many components. Seatools bv. supplied the industrial real-time computer, laptops and remaining electrical components for the setup. A general overview of all the used components and connections of the experimental setup is shown in Figure 29.

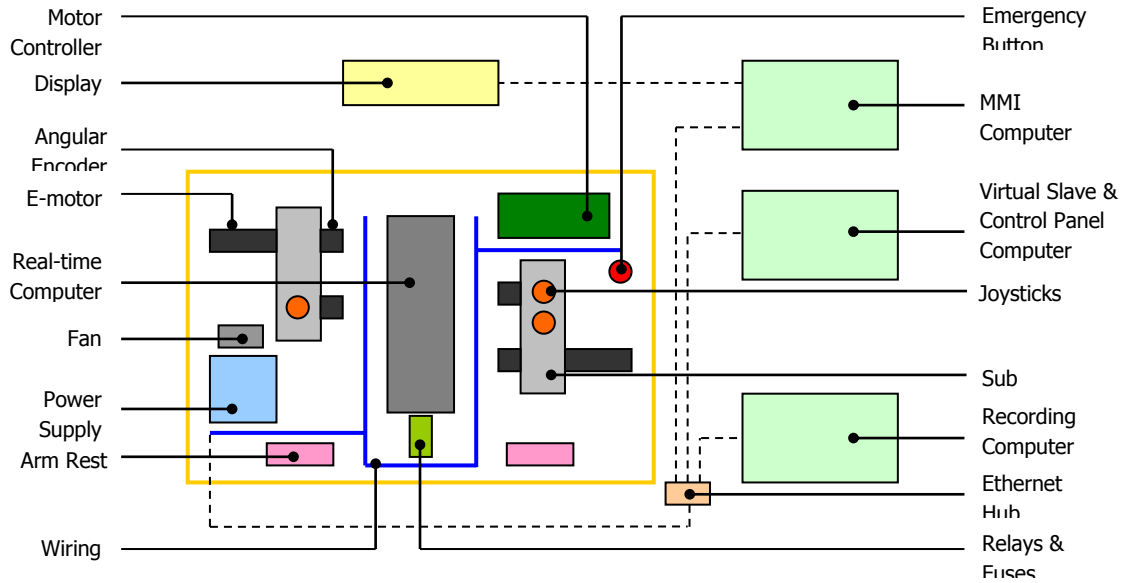

Figure 29: Schematic view of mechanical and electrical components of experimental setup

3.2.1 Mechanical

The mechanical components as shown in Figure 29 of the experimental setup are summarized listed in Table 9.

Description	Supplier	Details
Pulleys	DUT	Special pre-designed cable pulleys and cables
Springs	DUT	Inclusive modified spring stops and adjusters
Frame	Fabricated	Frames, handles and attachments

Table 9: Description of mechanical components of the experimental setup and their suppliers.

3.2.2 Electrical

The electrical components of the experimental setup are listed in Table 10. The real-time computer is powered trough the 24V power supply, also powering the motor control board. The real-time computer uses an analogue output to send a control signal to the motor control board, controlling the DC electrical motors with a pulse width modulation signal. The emergency button switches off the motor control board and therefore disabling the electrical motors, but the real-time computer remains powered.

Description	Supplier	Manufacturer	Details
Electrical motor	DUT	Maxon	RE35 90W 24V DC, GP32 planetary gearbox
Angular encodes	DUT	Scancon	2RMHF 7500 pulses incremental encoder
Real-time computer	Seatools	Bachmann	MX213, 200 MHz
Signal IO	Seatools	Bachmann	AIO288, DIO232 and 2xCNT204
Motor control board	DUT	AMC	2x az12a8ddc
Power Supply	Seatools	Puls	24V, 10A, 288 W
Cooling Fan	Seatools	-	-
Emergency button	Seatools	-	-
Relays and wiring	Seatools	-	Including contact detection hall sensors

Table 10: Description of electrical components of the experimental setup and their suppliers.

3.3 Software Design

Several software applications are designed for this experimental setup. An interface is designed for visualizing the process parameters to the operating and enabling communication of the operator to adjust settings of the process, using a Man-Machine Interface (MMI) as described in paragraph 3.3.2. A local controller is designed to operate the master device and apply the correct forces on the joysticks, as described in paragraph 3.3.3. The behaviour of the slave is calculated using a mathematical model as described in paragraph 3.3.4. All these software part communicate through the real-time computer, using a Standard Variable Interface (SVI) as described in the general overview in paragraph 3.3.1. A control panel is designed to apply the correct settings and experimental conditions, as described in paragraph 3.3.5.

3.3.1 General Overview

The general layout of the software structure is shown in Figure 30. This figure shows the three main software components connected with the SVI layer on the real-time computer; The MMI, virtual slave and local controller. Also two less important software components are shown, the control panel to adjust settings and the recorder for offline analyses.

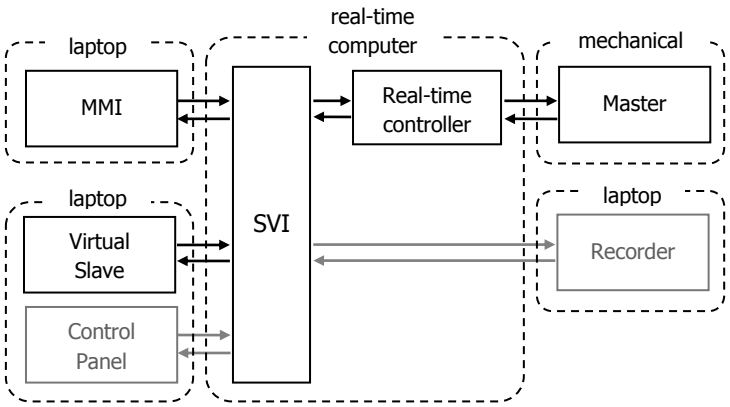

Figure 30: Software structure of the experimental setup

Three laptops are connected with the real-time computer using a hub as shown in Figure 29. Two extra displays were needed to display the MMI to the operator and one for the virtual model. Three laptops were needed for this setup as shown in Figure 30 and Figure 25, because of the loading and related stability of the software components. Due to the limited time to develop this setup, the MMI was programmed using Matlab GUI, causing unnecessary large process time running the program due to its Java machine. The virtual model on the other hand consists of just a large amount of computations, causing a large process time and

therefore the need to split these processes. The control panel was designed to run parallel on the same laptop as the virtual slave process. A third laptop was needed to run the recording program, to insure a stable recording of the measured variables.

3.3.2 Visual Interface

The operator is presented with a display that shows visual information about the deep sea mining process. The interface contains the position and some control parameters of this process, as shown in Figure 31. On the right bottom of the figure a top view of the grab is shown with several targets displayed, scheduled for excavation. These targets are linked to the tasks to be performed and help to execute them in the correct order. In the right top of the figure a side view of the operation is shown, to give a general overview of the process. The red dotted line represents the virtual start/finish line of the task, to compare experiment results and production calculation. On the left top of the figure is shown the relative position of the clamshells to the grab's frame. For each clamshell also the rotating velocity and hydraulic cutting force is shown in bar graphs. Some extra numerical data is shown in this field, indicating the progress of the excavation process. The button labelled with 'open grab' indicates whether or not the clamshells are controlled to be opened. This opening function is activated using the hardware button on the grasping joystick, but can also be activated in the MMI.

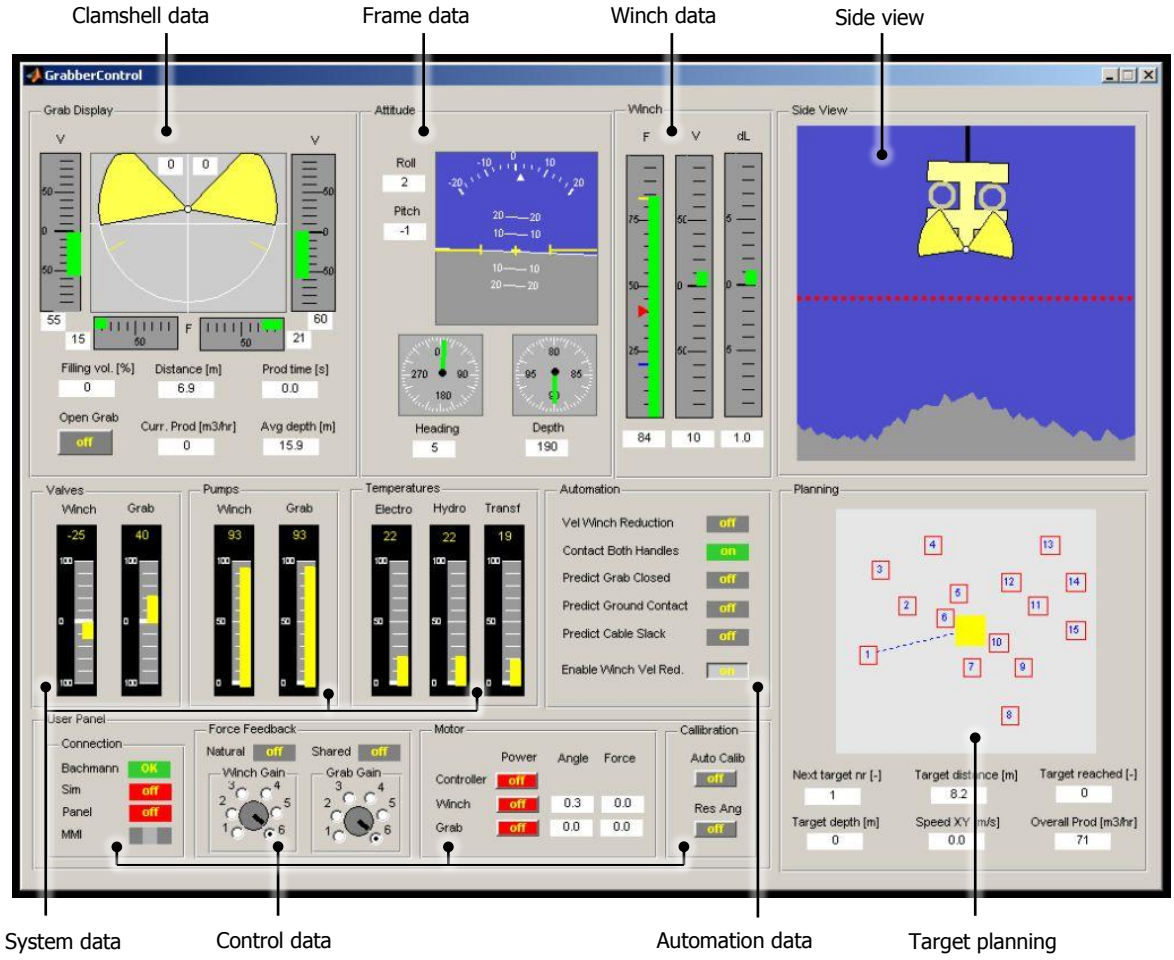

Figure 31: Visual interface for controlling a deep sea mining process

The top middle part of the figure shows an artificial horizon, displaying the rotations of the grab's frame and two clocks display the heading and depth of the frame. Three bar graphs indicate the winch data, hydraulic cable force, velocity of the winch and the relative length. In Figure 32 is shown the principle of this relative

cable length as a difference in positions. The relative length variable displays whether the cable is stretched or has slack, indicating the expected reaction time of the cable force and frame displacement. The winch cable force bar also has an indication of the automatic controller showing the optimal cable force, displayed with the red triangle.

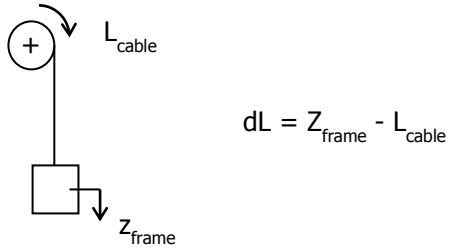

Figure 32: Relative cable length

In the left middle part of Figure 31 is shown some system data of the virtual grab, valve position, pump pressures and temperatures. On the right of this system data are some indicators, showing a five second prediction of some control actions. The bottom part of the interface displays some data of the experimental setup, such as connections and motor actuations.

3.3.3 Real-time Controller

The real-time controller determines the forces acting on the mechanical setup. The controller uses the angular incremental encoders and the setpoint data from the virtual model to control the electrical motors of the setup. The controller consists of two parts as shown in Figure 33 b), one for the winch and one for the grab joystick, both almost identical. The main difference between both controller parts is the bidirectional movement and therefore switching of the force direction and the detection of the mid position. The in- and outputs of both control parts is read and written to the SVI layer on the real-time controller as shown in green in Figure 33 a).

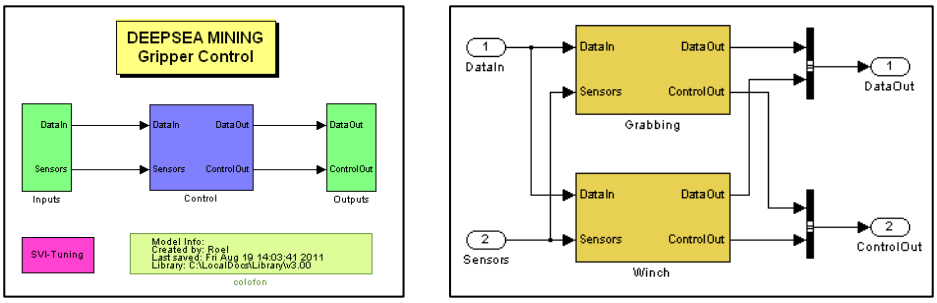

Figure 33: a) Top level of control model as implemented in Matlab Simulink. b) Control of the real-time controller, showing two control parts for the grasping and winch joystick.

The general overview of a control part is shown in Figure 34, where the grabbing control part is displayed. The control part contains a logic part, checking sensor signals, directions, temperatures and standby functions. The calibration part initializes the incremental encoders and has an automatic calibrations function. The length and forces of the springs and force on the handles is calculated in the setup part of the control, for offline analysis and not for controlling the forces. The force setpoint part of the control calculates the required force based on the joystick angle, settings of the experiment and the setpoint from the virtual grab simulation. The output control to the motor is calculated in the controller with the use of feed forward, calculated from the setpoint. This is included with output limitations, protections and calibration of the output motor signal. The feed forward control is found the most stable control instead of several applied closed loop controls, based on angular feedback from the motors and joysticks. The calculated forces of the springs with

their hysteresis in combination with the backlash in the gears mainly caused this instability of the closed loop controls.

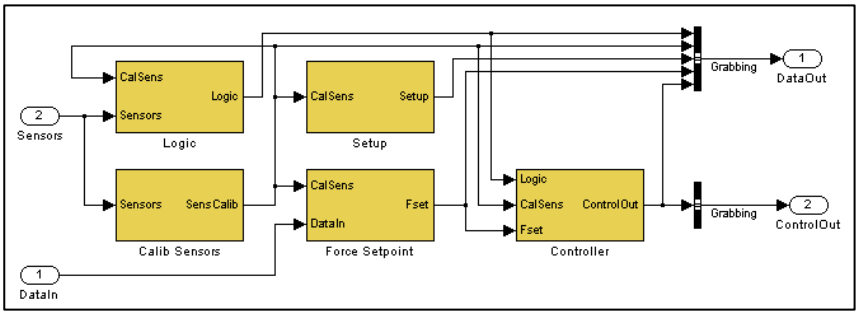

Figure 34: A Matlab Simulink representation of the grabbing control part of the real-time controller

The mathematical model of the virtual slave sends the main setpoint for transparent feedback to the control model, based on measurements of the virtual hydraulic pressure. The setpoint for haptic shared control also comes from the virtual grab model, based on several conditions of the system such as cable force and predicted ground contact. The actual force setpoint for motor actuation of the joystick is calculated based on these setpoints as shown in Figure 35. The setpoint is based on a minimal static force, a spring force calculated using the angle of rotation and an end force. The control force is not used during this experiment and was added for calibration purposes. The vibration forces are added to the force setpoint with some limiting checks finally for ensuring safety of the system.

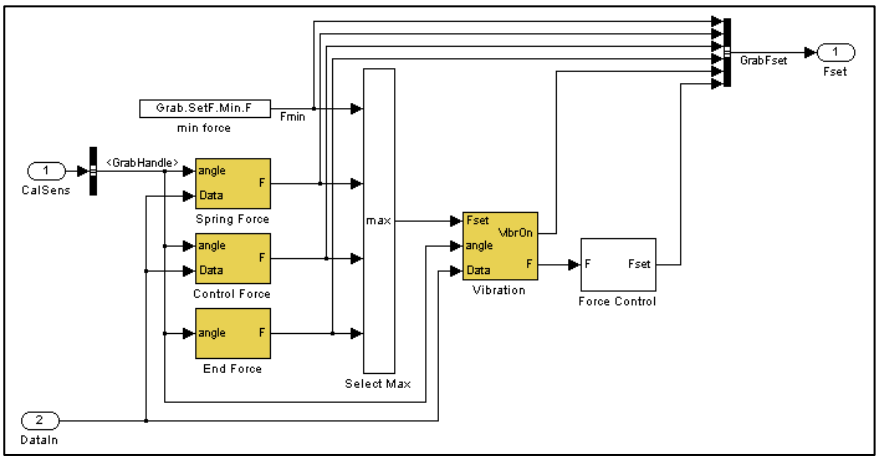

Figure 35: Matlab Simulink representation of force setpoint calculation, depending on different components

The method of applied feedback mechanisms is schematically shown in Figure 36 a) for the winch joystick and in Figure 36 b) for the grab joystick, displaying the return force against the joystick angles. The minimal returning force (F_{min}) is present in all conditions to return the joysticks to their initial position. Variable spring stiffness is applied for natural feedback, adjusted proportional with the slave stiffness. The end of the stroke is marked with a force barrier in combination with a vibration alarm, when shared control is enabled. The winch feedback is identical to the grab feedback, only the winch feedback is applied in both directions and the grab feedback only has one direction.

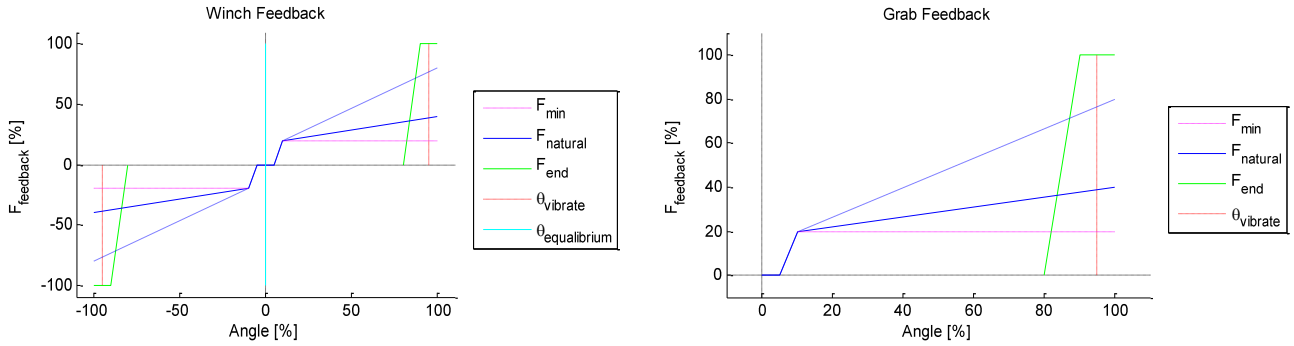

Figure 36: a) Illustration of the force feedback mechanisms of the winch joystick. b) Illustration of the force feedback mechanisms of the grasping joystick.

In Figure 37 is the actual shared control feedback mechanism shown, which essentially calculates the optimal steering angle, and then shifts the equilibrium point of the joystick to that angle. A changed force is applied due to the shift of equilibrium point, if the joystick remains in the same position, causing a pull to this new point. Contact detection using hall sensors inhibits the joysticks to rotate when the operator does not hold the joystick. Furthermore to induce the need for the operator to participate in the movement, is the applied new control position always slightly less than required. The shifting of the equilibrium point guides the operator to the correct control position of the joysticks and the force end barrier acts as a virtual fixture of the joystick.

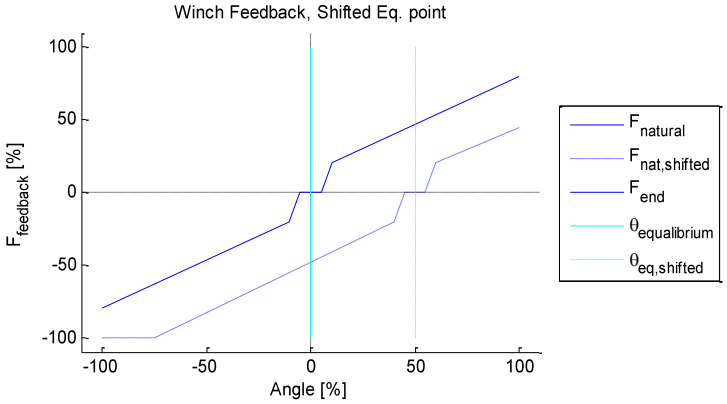

Figure 37: Illustration of the mechanism of shifted equilibrium point of the continuous haptic shared control feedback mechanisms for the winch joystick.

3.3.4 Virtual Grab Simulation

Using an actual slave robot during this experiment was not an option and therefore a virtual slave robot had to be designed. A mathematical simulation model is developed for calculating the behaviour of this virtual grab. Figure 38 shows the top level view of this simulation for the behaviour of a grab. The in- and outputs of the simulation are level-2 S-functions for implementing the communication protocol with the real-time controller, using a special developed script by Seatools bv. for establishing this communication using the Transmission Control Protocol (TCP).

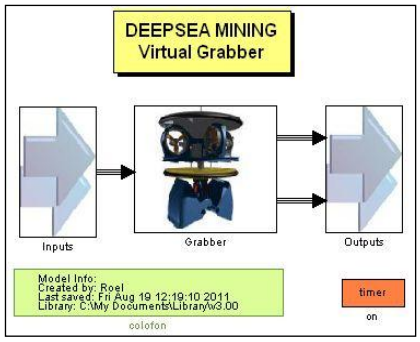

Figure 38: Top level of Matlab Simulink representation of the virtual grab model.

The general in- and outputs to and from the virtual grab simulation are given in Figure 39. The control panel transfers setting to the virtual slave for experimental conditions and task numbers to be executed. The user controls the master device, which sends the angular values to the controller which again sends its calibrated values to the virtual grab simulation that controls hydraulic valves. The haptic feedback settings to the controller are set by the virtual grab simulation and the visual feedback on the display is based on the behaviour of the virtual grab from the simulation.

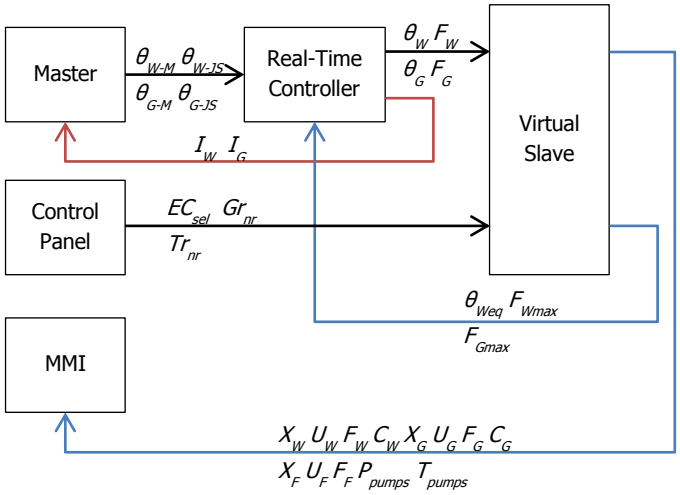

Figure 39: Schematic view of communication of the virtual grab model.

The calculation of the behaviour of the virtual grab is subdivided into physical separated parts, illustrated in Figure 40. The generated ship motions after heave compensation induce a change of position of the winch drum. The control signal from the winch joystick adjusts the position of a hydraulic valve, controlling the velocity and force of the winch drum. The cable force acts backwards on the winch drum but is also dependent on the relative winch and frame position, causing a spring force.

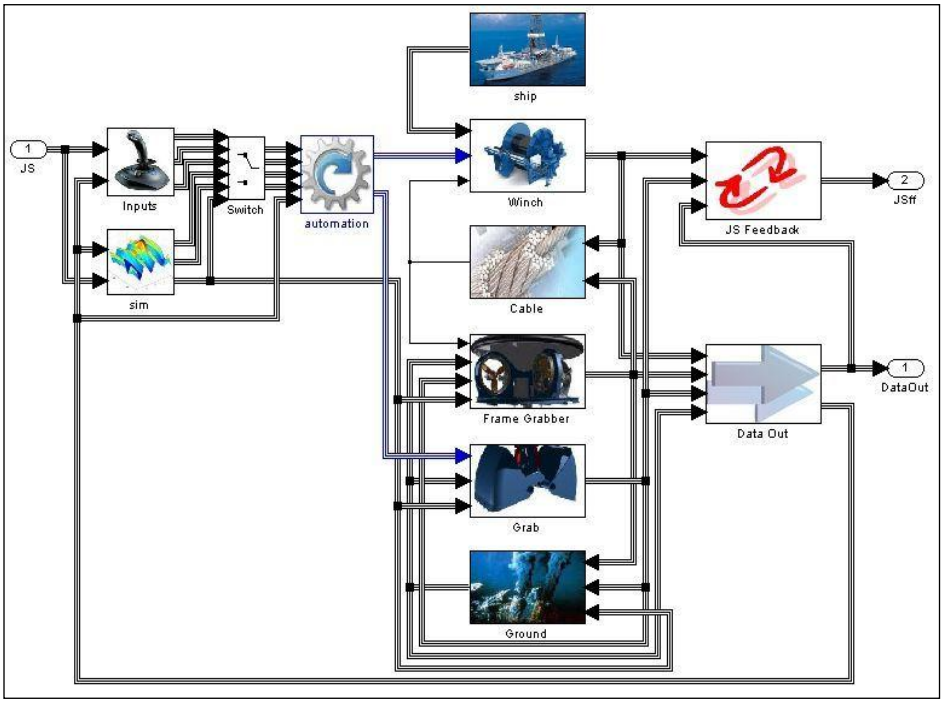

Figure 40: A Matlab Simulink representation of the virtual grab simulation model, subdivided into physical separated parts.

Figure 41 illustrates the calculation of the frame position from the various forces acting on it. The frame calculation mainly consists of a six degree of freedom (DoF) mass with four forces translating and rotating it. The thruster force is controlled with an automatic controller for holding the horizontal position and rotation around the z-axis constant during free hanging. The cable force is decomposed in a vertical and horizontal component in combination with momentum acting on the frame. This calculation is done using rotation matrices from the Euler angles for converting the inertial components to body components. This conversion is done for all four forces.

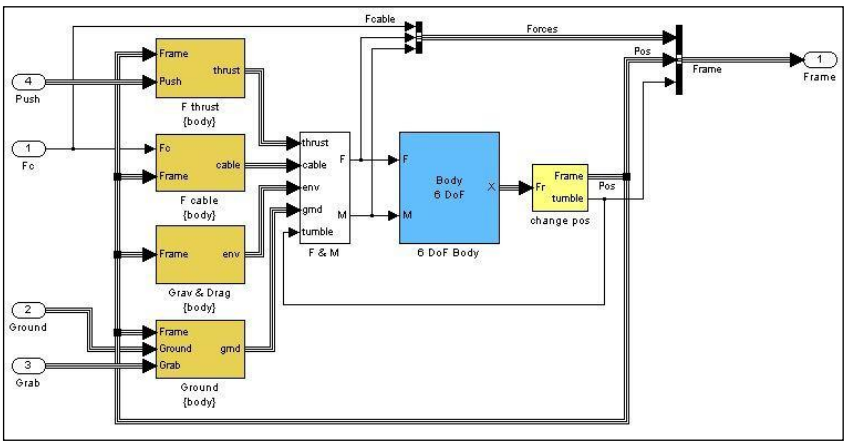

Figure 41: A Matlab Simulink representation of the calculations of the grabs frame dynamic behaviour.

The position of the frame is combined with the relative translation of the clamshells. The translation of the clamshells is subdivided into a hydraulics part and translation part, comparable to the winch calculation. The control signal from the grab joystick manipulates a hydraulic valve as well. The clamshells are actuated with hydraulic cylinders consisting of changing compressible hydraulic volumes. The hydraulic flow can be calculated from a simple pump simulation in combination with this valve position. The forces of the

clamshells are acting on the ground causing the rock material to break. The subdivision of the calculations for reaction of the ground forces is shown in Figure 42 a). The simulated ground pattern as also shown in the visualization, is first calculated for the position of the ground level. From this position and the clamshell positions, contact can be determined. When contact is enabled, the calculation holds contact for stability of simulation. Contact is broken if vertical forces exceed a threshold for a certain time. The reacting ground forces are modelled as a spring-damper for both teeth positions of the clamshells in both horizontal as vertical direction as shown in Figure 42 b). Therefore the ground forces are in equilibrium with the frame and clamshell dynamics, so mainly gravity and inertial reactions. The cutting forces are calculated as the resulting sum of all ground forces and clamshell forces. These cutting forces are used to determine the breaking of rock chips, using a vector of thresholds to determine fracturing of the rock material. When a threshold of rock forces is exceeded, the contact position of the rock is changed at a limited rate.

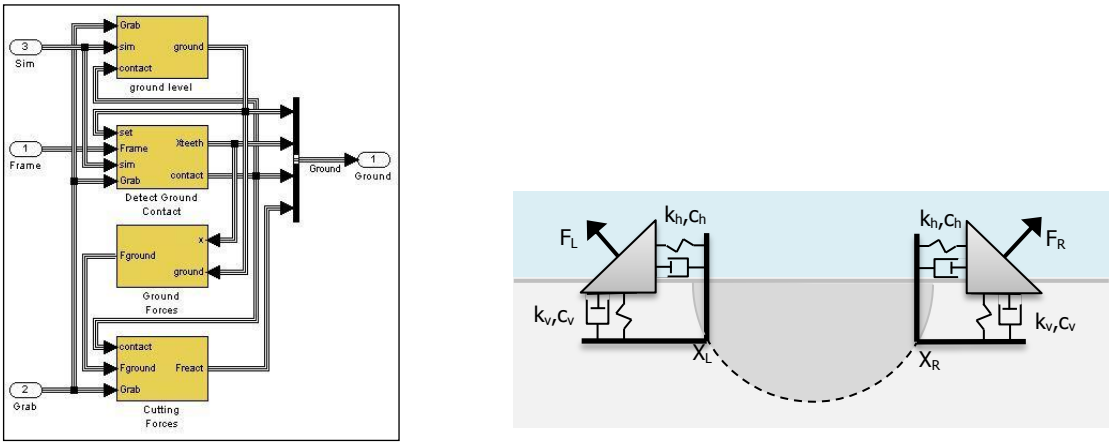

Figure 42: a) A Matlab Simulink representation of ground contact and force calculations. b) Schematic representation of mass-spring system for ground contact forces for changing ground positions.

The setpoints of the feedback forces for the mechanical setup are calculated from all the calculated positions and forces of the virtual grab. The setpoint for the natural force feedback is simply proportional to the hydraulic pressure of the actuator. The calculation of the equilibrium point for shared control on the winch joystick is shown in Figure 43 as previously described and shown in Figure 37 in paragraph 3.3.3. The setpoint is calculated based on contact with ground, cable force, failure of components and the position of the clamshells. These values are based on a five second prediction calculated with the velocity of these values. The calculation of the setpoint for the cable force is based on the prediction of contact, rotation of the frame and closing of the clamshells. This setpoint is also transferred to the visualization to help the operator controlling the process.

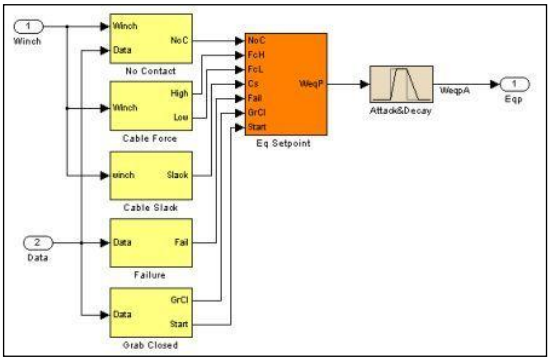

Figure 43: Calculation of equilibrium point for winch shared control

Non-linear control output

The virtual grab is controlled with the use of two joysticks; one for rotating the winch drum and therefore controlling the cable force, and one joystick for rotating the clamshells and therefore the grab force. Both joysticks operate a hydraulic valve of the virtual slave, therefore controlling the velocity or force when there is load on the actuator. The winch joystick handle has a non-linear output character to the given rotation angle of the joystick, as shown in Figure 44 a). This increases the sensitivity of the control while still enabling full speed of the controlled actuator.

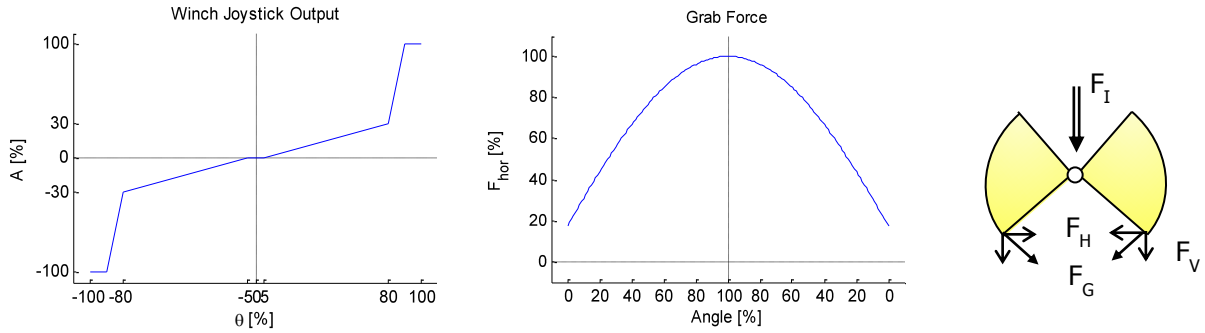

Figure 44: a) Non-linear winch joystick output b) Non-linear grab force c) decomposed grab forces.

The output grab force has a non-linear character as shown in Figure 44 b), due to the geometry of the clamshells rotating on the frame. The output force can be decomposed into a vertical and horizontal component, as shown in Figure 44 c). The vertical component is limited by the weight and dynamic effects of the entire grab and is therefore relative small. The horizontal force increases when the closing angle increases; therefore the available grab force increases while closing the grab.

3.3.5 Control Panel

A simple control panel is designed for determining the settings for the experiment and overview the setup, shown in Figure 45. An overview of the main parameters of the virtual grab simulation is shown real-time low frequent on the left of the panel. This also includes a check of the selected ground model, reaction forces and feedback mechanism. On the right of the panel is an overview shown of all the experimental setup parameters. The right bottom of the panel contains the selection of the force feedback mechanisms and task selection options. The centre of the panel contains the parameters and selections of the real-time control model.

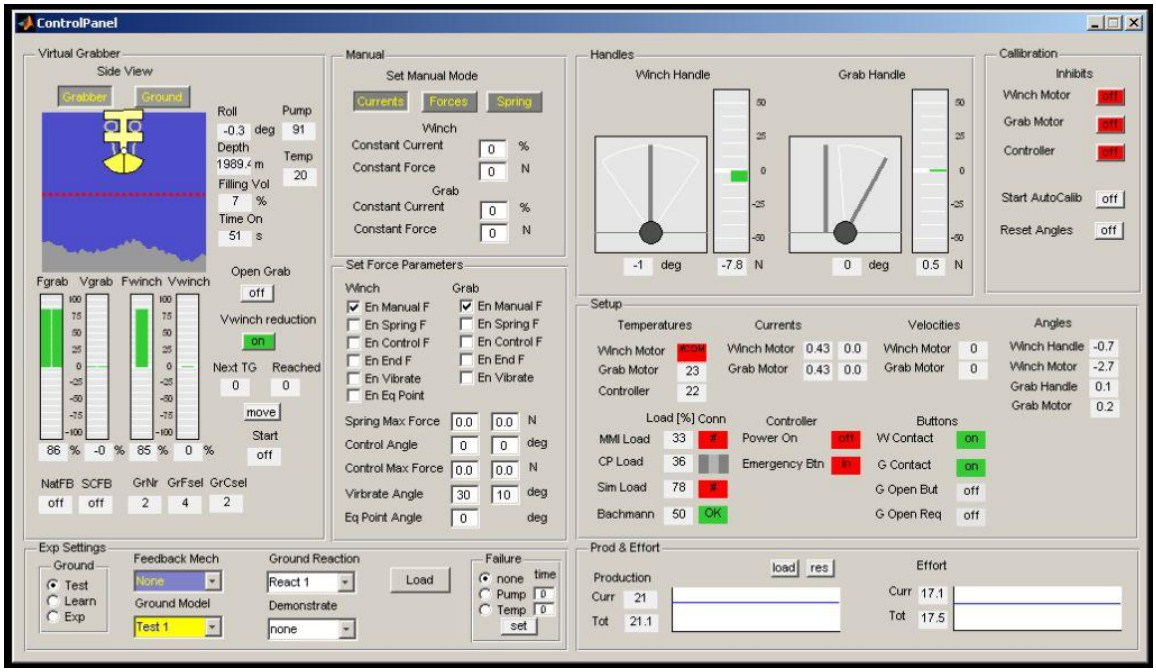

Figure 45: Control Panel

4 EXPERIMENT RESULTS

The experiment as described in chapter 2 was conducted to validate the hypotheses as described in paragraph 1.5. The hypotheses state improvements of performance for offering haptic shared and/or natural force feedback, reduction of control effort for when offering haptic shared control and increasing situation awareness when offering natural force feedback. The experiment was conducted at four experimental conditions as described in paragraph 2.2.1.; baseline condition direct control (DC), haptic shared control (DC-SC), natural force feedback (FF), both feedback mechanisms (FF-SC). The general results of the experiment are presented in paragraph 4.1 for the overall production results for all performance trials. The general results are also further elucidated by presenting several time traces of the experiment, and by presenting subjective results. The results during the three performance trials are analysed in more detail in paragraph 4.2, using the all described metrics as listed in Table 7 in paragraph 2.2.2. Statistical results of the catch trials with a reduced number of metrics are given in paragraph 4.3, only given for relevant metrics as described in paragraph 2.2.2.

4.1 General Results

Since the goal of the experiment for each subject is to excavate as much rock volume as fast as possible, the general performance is therefore defined as the gained rock volume divided over the time to complete, as previously described in paragraph 2.2.2. The individual results of the three performance trials for each subject for all four experimental conditions are shown in Figure 46 a), with the mean of all three performance trial per subject per condition and standard deviation. The means of all subjects per condition are separately shown in Figure 46 b) in combination with the overall mean of all subjects. However no conclusions can be drawn directly from both Figure 46 a) and b) due to the spread in results.

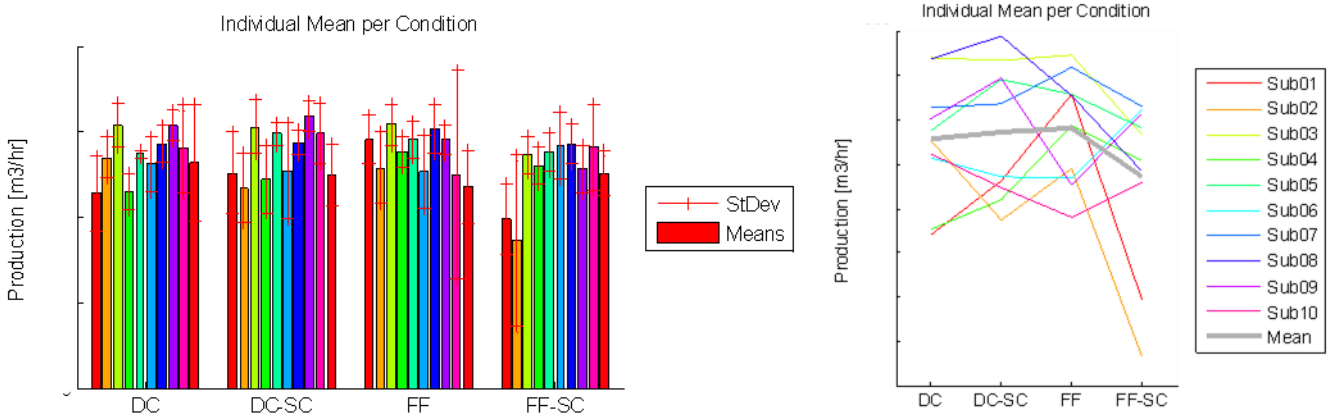

Figure 46: a) Mean and standard deviation of individual production results of performance tasks only, for each subject per experimental condition. b) Mean of production results for each subject of performance task and overall mean, for each experimental condition.

Mainly during catch trials time penalties were given for incorrect control of the virtual slave robot, based on large heeling angles or late response to critical situations as described in paragraph 2.1.3. The number of time penalties for each task at each condition, summated for all subjects are given in Figure 47. The first three tasks are the performance trials and the last three are catch trials as described in Table 5 in paragraph 2.1.3.

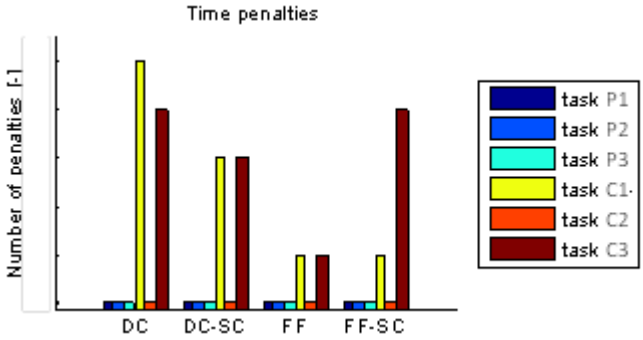

Figure 47: Results of number of time penalties per task for each condition, as a summation of all subjects.

The statistical significance of all results of the metrics as listed in Table 7 in paragraph 2.2.2 are shown in Table 11, using (••) for p≤0.01, (•) for p≤0.05, (-) for p>0.05 for level of significance. The general performance results do not shown a statistical difference, only the reduced frame angle results for natural force feedback. The control effort however does show some statistical significant reduction. The subjective workload is significant reduced for almost all conditions and subject rating increased for all conditions. The results workload and rating are given for all six tasks. The results for frame angle, cable length difference and force deviation are given for the catch trial tasks. The other performance and control effort results are given for the three performance tasks.

	Trial	DC-SC	FF	FF-SC
Time	P1-3	-	-	•
Volume	P1-3	-	-	-
Production	P1-3	-	-	-
Frame Angle	C1	-	•	•
Cable Length Difference	C1	-	-	-
Force Setpoint Deviation	C1	-	-	-
Summation Joystick Angle	P1-3	••	-	••
Moving Joystick Angle	P1-3	-	-	•
Applied Joystick Force	P1-3	••	••	••
Overall Workload	P&C1-3	-	•	••
Overall Rating	P&C1-3	••	••	••
Reaction Time	C3	-	-	-

Table 11: Two-way ANOVA results for all evaluation metrics compared to the baseline conditions DC, using (••) for p≤0.01, (•) for p≤0.05 and (-) for p>0.05. For each metric the corresponding trial is given, performance trials (P), catch trials (C), the number indicates the corresponding trial number.

Several results of control input and virtual slave responses using time traces are given in paragraph 4.1.1. Results of the self-assessment as described in Table 8 in paragraph 2.2.2 are given in paragraph 4.1.2.

4.1.1 Time Trace Results

The time trace results of one subject for all three performance tasks at every applied feedback mechanism are shown in Figure 48. This subject had the second best overall production results and was operating the system with the highest subtlety. The three subfigure of Figure 48 a) display the winch joystick angle over time for all conditions at each task. The winch joystick is controlling the rotation of the winch drum and therefore the cable tension during ground contact. The three subfigures of Figure 48 b) show the applied cable force and given setpoint of cable force for each condition at each task.

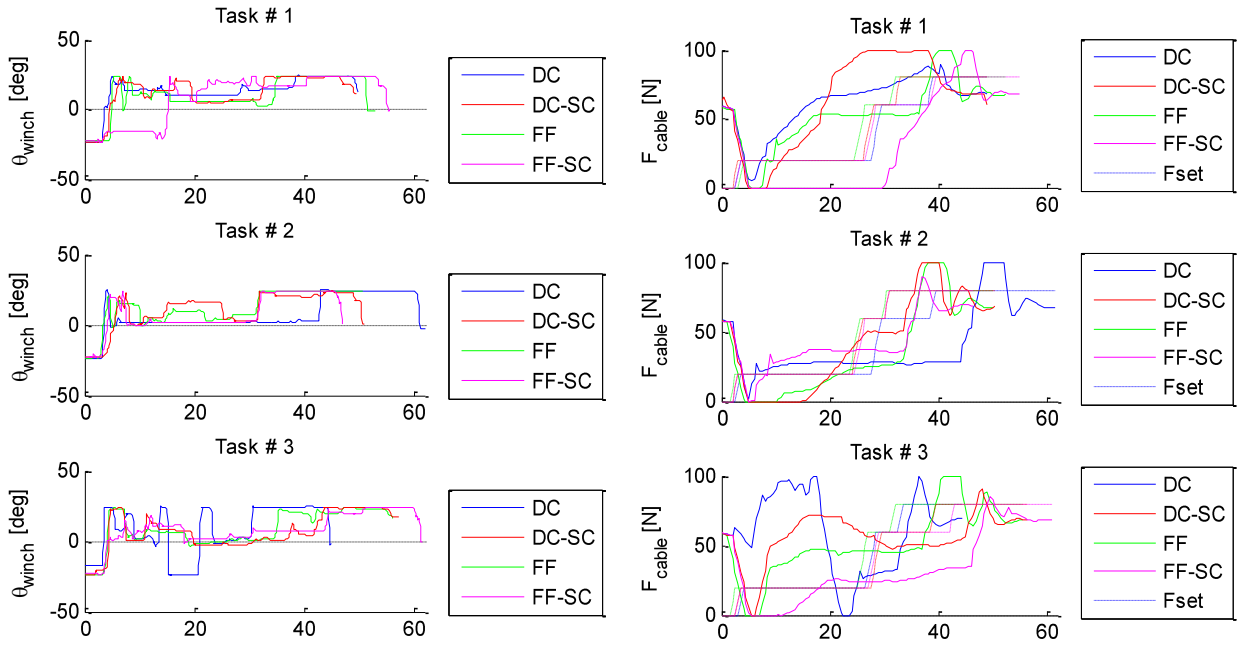

Figure 48: a) Time trace results of winch joystick rotation angles of subject nr.6 during all three performance tasks. b) Time trace results of cable tension force of the virtual slave robot simulation for all three performance tasks.

The time traces as shown in Figure 48 display different control actions and responses of cable forces of the virtual slave robot, even when controlling an identical task under different conditions. A more clear view of a single task of a typical control action with several response parameters of the virtual slave robot is shown in Figure 49 a) and b). The time trace is shown for subject nr.6 during performance task 1 using direct control (DC) in Figure 49 a) and haptic shared control (DC-SC) in Figure 49 b). Both figures show the control action compared to response of slave robot simulation for heeling angle of frame, force of cable and setpoint for cable force. In Figure 49 b) is shown also the setpoint for the haptic shared control feedback.

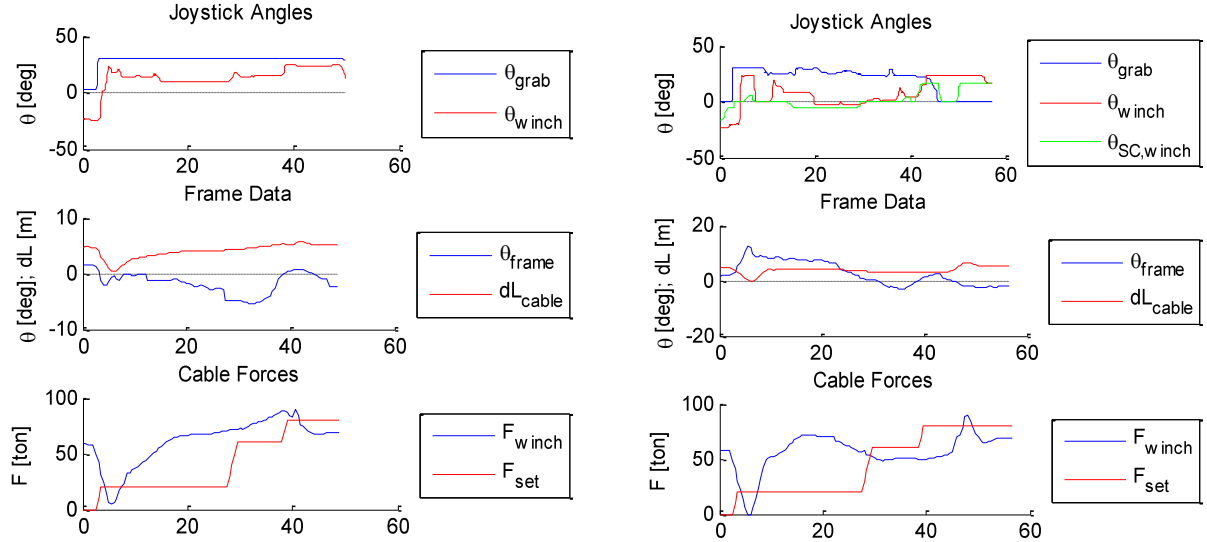

Figure 49: a) Time trace results of performance task 1 for subject nr.6 using direct control (DC) as experimental condition, showing the control action of joystick angles and reaction of the slave robot simulation of relative cable length, heeling angle and cable force with controller setpoint. b) Time trace results of performance task 1 for subject nr.6 with Haptic Shared control feedback (DC-SC) showing identical parameters, including the feedback parameter for the winch joystick.

Control actions using the joystick angles can be decomposed into a low and high-frequent control movement as shown in Figure 50, using a break-frequency of 0.1 Hz. Due to this breakup in frequency, the overall control movement of the subject is split from the short term control corrections of the subject. The high-frequent movements are an indication of the control effort of the subject to control the process.

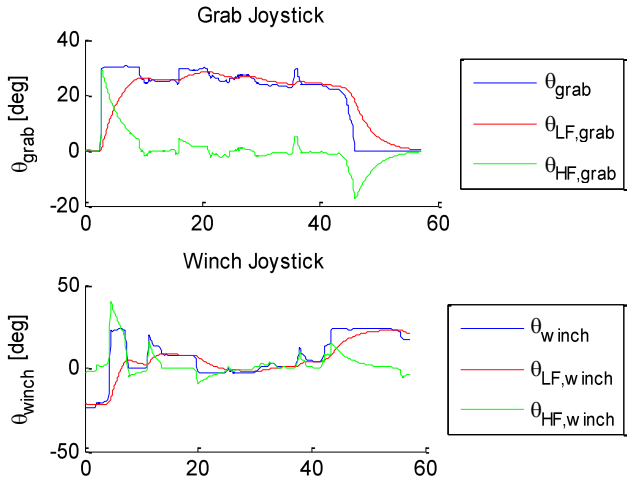

Figure 50: Decomposition of low and high-frequent control movement of joystick angles for subject nr.6 using haptic shared control (DC-SC) condition during performance task 1.

The time trace results show a large variation of control of the process, also within the same task as shown in Figure 48. It is therefore very difficult to draw conclusions from looking only at this time trace data. A statistical representation of the data is more effective to display an overall subtle trend in data results.

4.1.2 Self-Assessment Results

The statistical results of all six questions from the TLX assessment are shown in Figure 51. Almost all questions indicate a reduction of effort compared to the baseline condition. The haptic shared control (SC) conditions seem to decrease the effort more than natural force feedback (FF). Due to the small sample size of ten subjects these reductions are not always significant.

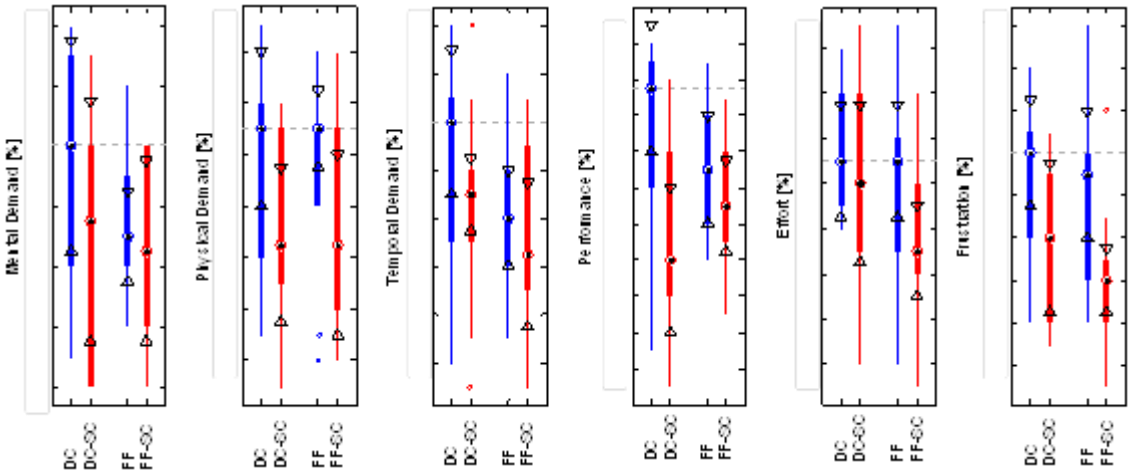

Figure 51: Self-assessment of all six workload metrics, shown for all four experimental conditions in each graph.

A two-way ANOVA is performed on all results to state the statistical significance for equal mean corrected for in between subject differences, given in Table 12. Not all results have statistical significant ($p \leq 0.05$) different means.

Condition	MD	PD	TD	PE	EF	FR
DC : DC-SC	-	-	-	•	-	-
DC : FF	•	-	•	-	-	-
DC : FF-SC	-	-	•	-	••	•
DC-SC : FF-SC	-	-	-	-	-	-
FF : FF-SC	-	-	-	-	-	•

Table 12: Two-way ANOVA results for difference in means of all six self-assessment questions, using (••) for p≤0.01, (•) for p≤0.05 and (-) for p>0.05 significance level.

The overall workload is the combination of all six questions with even weighing. Each subject was also asked to give a rating of the entire experience of the experimental condition. These statistical results are shown in Figure 52. The results indicate an increase in overall rating for all conditions compared to the baseline condition (DC) and a decrease in workload. The difference in the mean of results are enlarged for both conditions with haptic shared control applied (SC).

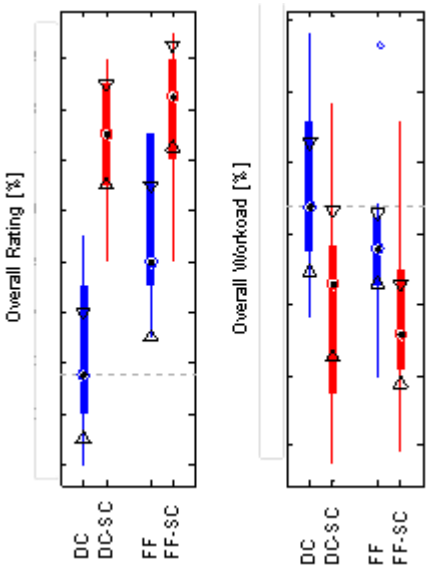

Figure 52: Overall workload and rating results,

The statistical significance level of the difference in means as shown in Figure 52 is listed in Table 13. The results show for almost all conditions a statistical significant (p≤0.05) difference in means compared to the baseline condition.

Condition	Overall Rating	Overall Workload
DC : DC-SC	••	-
DC : FF	••	•
DC : FF-SC	••	••
DC-SC : FF-SC	-	-
FF : FF-SC	••	••

Table 13: Two-way ANOVA results of overall self-assessment, using (••) for p≤0.01, (•) for p≤0.05 and (-) for p>0.05 significance level.

4.2 Performance Trials

The six tasks to be executed for each condition consist of three performance tasks and three catch trials as described in Table 5 of paragraph 2.1. During the three performance tasks per condition, the subject was operating the system under normal conditions. Results of these tasks are given in the time and statistical domain to analyse the difference of feedback mechanisms. Paragraph 4.2.1 shows the results for the performance and system evaluation metrics, paragraph 4.2.2 the results of the control effort metrics. The evaluation metrics of the self-assessment is only given in paragraph 4.1.2 for all six tasks combined as general results, due to the subjective nature of the questions.

4.2.1 Performance and system results

This paragraph shows the statistical performance and system results of the performance trials as described in the list of evaluation metrics in Table 7 in paragraph 2.2.2.

Performance Results

The statistical results for production time, production volume and resulting production of all three performance trials are shown in Figure 53. The results only show a slight increase of time to complete for both feedback mechanisms FF-SC and therefore show a slight decrease of production results as well.

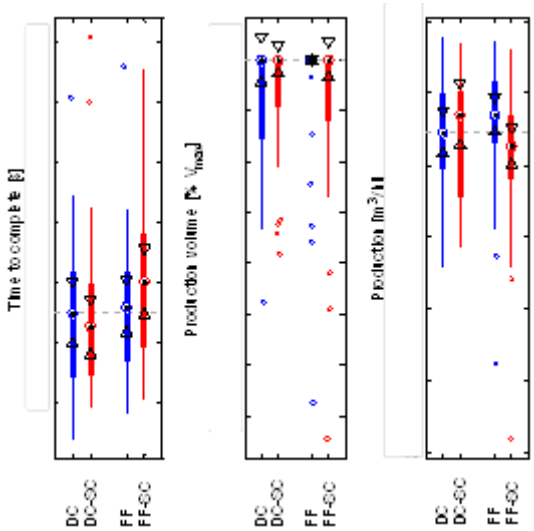

Figure 53: Production results absolute and normalized with the control condition median

The statistical significance level of the difference in means of the results as shown in Figure 53, is given in Table 14. The results show hardly any significant difference in means compared to the baseline condition DC.

Condition	Time	Vol	Prod
DC : DC-SC	-	-	-
DC : FF	-	-	-
DC : FF-SC	•	-	-
DC-SC : FF-SC	•	-	-
FF : FF-SC	•	-	-

Table 14: Two-way ANOVA results of performance data, using (••) for p≤0.01, (•) for p≤0.05 and (-) for p>0.05 significance level.

System Data Results

The heeling angle of the grab's frame is an indication of the effective level of control of the operator. If the cable force in combination with the rock cutting force at critical moments is not correct controlled, the heeling angle will increase. A warning is given to the operator when exceeding a minimum level of of heeling absolute and a maximum angle for causing an error, as described in 2.1.3. The attention of the operator can be measured by the magnitude of slack of the cable. The magnitude of deviation from the given optimal cable force setpoint is an indication of the correct response of the operator for controlling the process. These three described variables are shown in Figure 54. The maximum heeling angle of the grab's frame increases slightly when haptic feedback is applied, but the spread in data is very large compared to the differences. The maximum slack of the cable has a large spread as well and a very small difference in means. The deviation of cable force from the controller setpoint is almost the same for all conditions combined as well with a large spread in data.

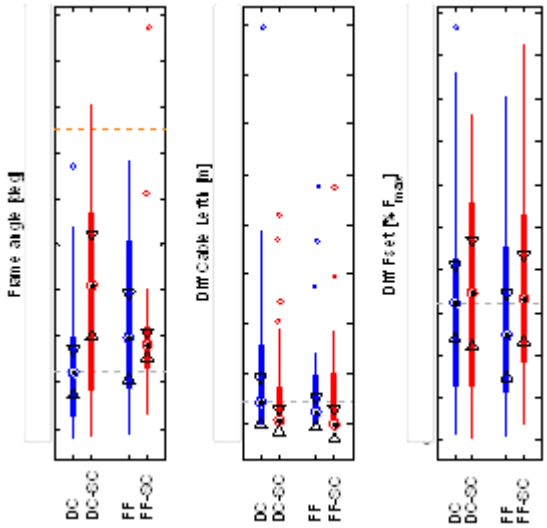

Figure 54: Results for maximum heeling angle of frame, maximum slack of cable and average deviation of cable force from setpoint. The orange dotted line in the frame angle results shows the warning level of heeling.

The levels of statistical significance of the results as given in Figure 54 are listed in Table 15. Only the frame angle shows statistical difference in means, however it indicates an increase in mean.

Condition	Frame Angle	Diff Lcable	Diff Fcable
DC : DC-SC	••	-	-
DC : FF	••	-	-
DC : FF-SC	-	-	-
DC-SC : FF-SC	-	-	-
FF : FF-SC	-	-	-

Table 15: Two-way ANOVA results of system data, using (••) for p≤0.01, (•) for p≤0.05 and (-) for p>0.05 significance level.

4.2.2 Control Effort Results

This paragraph described the total summed joystick angle during a conducted task and high-frequent moving angle, indicating the control effort of the subject.

Sum Angle Results

The sum angle is the average joystick rotation angle during an entire task, indicating the amount of joystick usage per condition. The statistical results are shown in Figure 55 for each individual joystick and an average of both joystick angles, shown for all three performance tasks for every experimental condition. The results indicate a large reduction of joystick usage for the grab joystick, when applying haptic feedback. The use of the grab joystick especially reduces when applying haptic shared control (SC). The cause of this reduction is the warning vibration on the grab joystick handle, when the clamshells are closed and a closing force is unnecessary. This effect is shown with a time trace for a subject with and without shared control in Figure 49 in paragraph 4.1.1. The operator holds on to the grab joystick during the entire task without feedback. With shared control the warning prevents the operator for unnecessary action with the joystick.

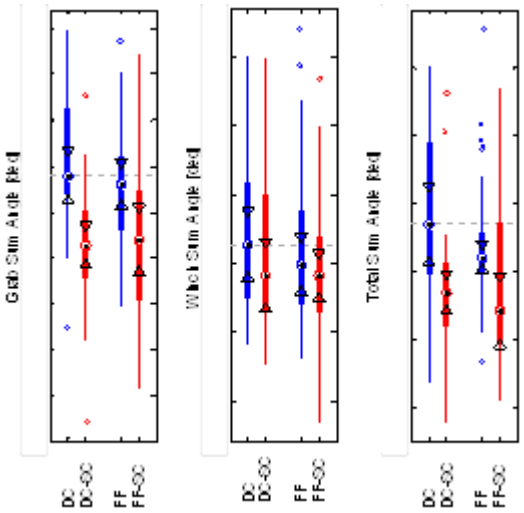

Figure 55: Average of rotation angle of joystick during entire task of the grab, winch and both joysticks average angles for all four conditions.

The level of significance is listed in Table 16, for the difference in means of the summed joystick angles as shown in Figure 55. The grabbing joystick angle and total angle show a statistical significant difference in means compared to the baseline condition DC.

Condition	Grab Sum Ang	Winch Sum Ang	Total Sum Ang
DC : DC-SC	••	-	••
DC : FF	•	-	-
DC : FF-SC	••	-	••
DC-SC : FF-SC	-	-	-
FF : FF-SC	•	-	••

Table 16: Two-way ANOVA results of total summed joystick angle, using (••) for p≤0.01, (•) for p≤0.05 and (-) for p>0.05 significance level.

Move Angle Results

Another indication for the operator's effort is the movement of the rotation angle and therefore the average of the high frequent rotation. The time trace results in Figure 50 in paragraph 4.1.1 show the decomposition of both joystick angles in a low and high frequent part, with a 0.1 Hz distinction. The statistical results for the average of this high frequent movement of the joystick angles are shown in Figure 56, for both joysticks individual and combined for all four conditions. The results do not show a noticeable difference for changing conditions, except when both feedback mechanisms are combined (FF-SC).

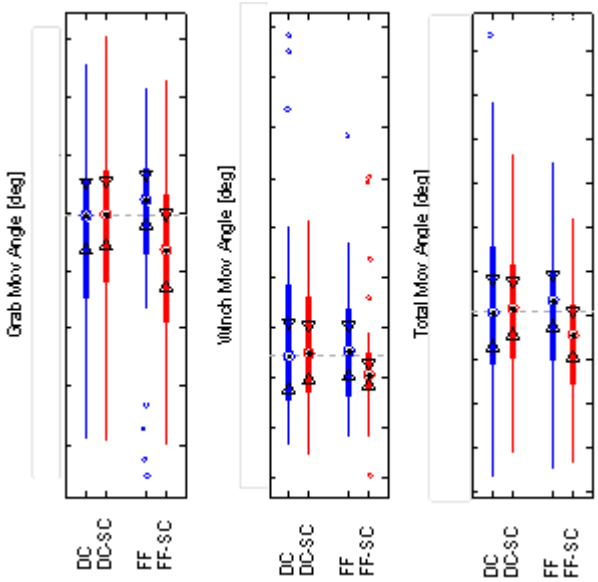

Figure 56: Statistical results of average high-frequent joystick movement of the grab, winch and both joystick angles for all four conditions.

Hardly any statistical level of significance is calculated for the results as given in Figure 56, which is shown in Table 17.

Condition	Grab Mov Angle	Winch Mov Angle	Total Mov Angle
DC : DC-SC	-	-	-
DC : FF	-	-	-
DC : FF-SC	-	-	•
DC-SC : FF-SC	-	-	-
FF : FF-SC	-	-	-

Table 17: Two-way ANOVA results of high-frequent moving joystick angle, using (••) for p≤0.01, (•) for p≤0.05 and (-) for p>0.05 significance level.

Applied Force Results

The statistical results of the applied forces on the joysticks are shown in Figure 57, as an objective indication of the physical load of the subject. The results clearly indicate the differences of applied forces for the feedback mechanisms. During the baseline condition (DC) hardly any force was applied besides a static small spring load as a return force to the initial position. The haptic shared controller (SC) shows an increased feedback force level, as explained in paragraph 3.3.3 and shown in Figure 36 a) and b).

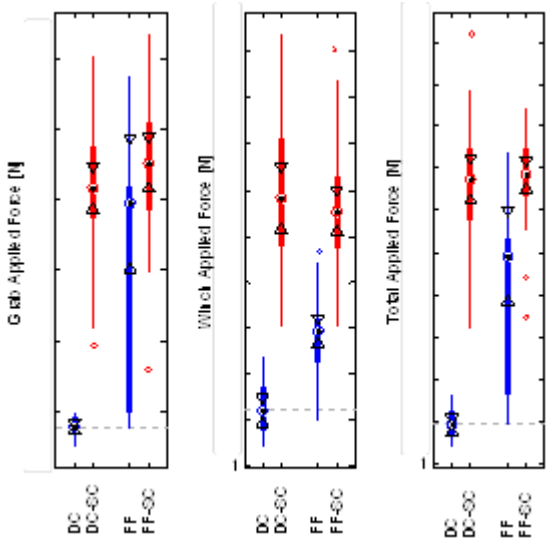

Figure 57: Statistical results of applied joystick force

The levels of significance are given in Table 18 for the applied joystick force as shown in Figure 57, all statistical significant different compared to the baseline condition DC where hardly any joystick force was applied.

Condition	Grab Fapplied	Winch Fapplied	Total Fapplied
DC : DC-SC	••	••	••
DC : FF	••	••	••
DC : FF-SC	••	••	••
DC-SC : FF-SC	-	-	-
FF : FF-SC	••	••	••

Table 18: Two-way ANOVA results of applied joystick force, using (••) for p≤0.01, (•) for p≤0.05 and (-) for p>0.05 significance level.

4.3 Catch Trials

Besides the three performance trials, three catch trials were conducted as well as described in paragraph 2.1.3 and listed in Table 5. The first catch trial was essentially more just a very difficult task to complete, due to hard soil conditions causing fast changing high reaction forces to the grab, statistical results shown in paragraph 4.3.1. However not all subjects completed the task due to the difficult conditions, resulting in zero production volume. The second trial was to increase the attention level of the subject and not expected to complete the task, due to very hard soil conditions exceeding the grab's capabilities, shown in paragraph 4.3.2. The third catch trial was to determine the reaction time of the operator after a mechanical failure, only visual noticeable. Only the statistical results of the reaction times are given in paragraph 4.3.3 of the last catch trial.

4.3.1 Catch Trial of Critical Situation

For this catch trial only the statistical results for performance, system data and a reduced number of results of control effort are given, as relevant information.

Performance Results

The statistical production results during this critical situation are shown in Figure 58, for time to complete, production volume and overall production. The results show a slight decrease in time to complete for the haptic shared control conditions (SC) and an increase for the natural force feedback conditions (FF). The large spread of the results is due to the small sample size and large variety in completion of task, due to abortion of the tasks of several subjects.

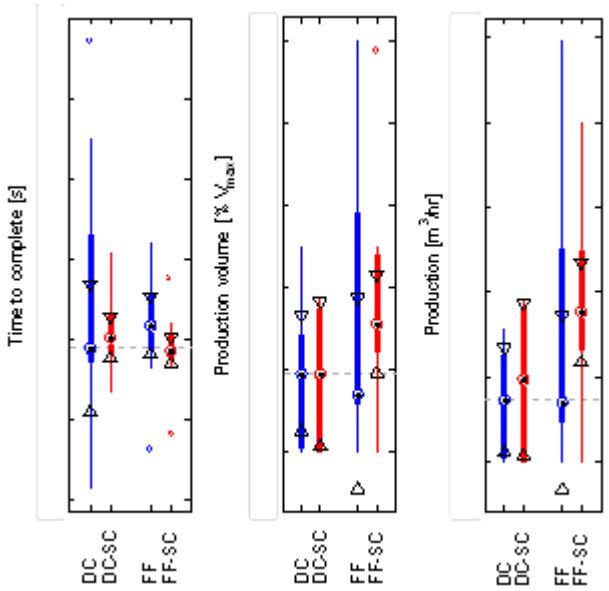

Figure 58: Statistical results of performance data for the catch trial of a critical situation, for all four experimental conditions.

Hardly any statistical level of significance is calculated for the results as given in Figure 58, which is listed in Table 19. Only the production results for both feedback mechanisms (FF-SC) compared to the baseline conditions (DC) show a statistical significant difference.

Condition	Time	Vol	Prod
DC : DC-SC	-	-	-
DC : FF	-	-	-
DC : FF-SC	-	-	•
DC-SC : FF-SC	•	-	-
FF : FF-SC	-	-	-

Table 19: Two-way ANOVA results of performance data for the catch trial of a critical situation, using (••) for p≤0.01, (•) for p≤0.05 and (-) for p>0.05 significance level.

System Data Results

The maximum heeling angle of the frame, slack of cable and deviation to cable force setpoint are shown in Figure 59 for the critical situation catch trial. The results show a decrease of maximal heeling angle of the grabs frame when natural force feedback (FF) is applied.

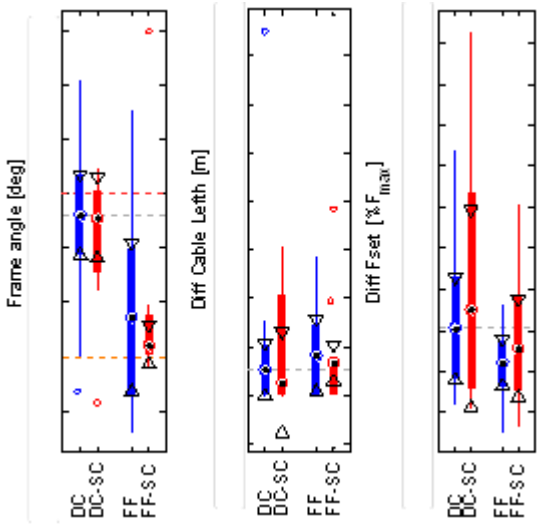

Figure 59: Maximum frame heeling angle, maximum cable slack and difference of cable force for the catch trial of a critical situation, for all four experimental conditions.

Only the results of the maximal heeling angle of the grabs frame shows statistical significant difference for all applied conditions compared to the baseline, as listed in Table 20. The results in Figure 59 for heeling angle show clearly a large reduction when applying natural force feedback during this difficult task, indicating a much improved situation awareness.

Condition	Frame Angle	Diff Lcable	Diff Fcable
DC : DC-SC	-	-	-
DC : FF	•	-	-
DC : FF-SC	•	-	-
DC-SC : FF-SC	•	-	-
FF : FF-SC	-	-	-

Table 20: Two-way ANOVA results of system data for the catch trial of a critical situation, using (••) for p≤0.01, (•) for p≤0.05 and (-) for p>0.05 significance level.

Control Effort Results

Statistical results for the average joystick rotation angle and the high-frequent movement of the rotation angle are shown in Figure 60. Both sum and moving angle do show a slight decrease of control effort compared to the baseline condition. The results for the applied joystick forces are comparable to the performance trials and therefore irrelevant and not shown for this task.

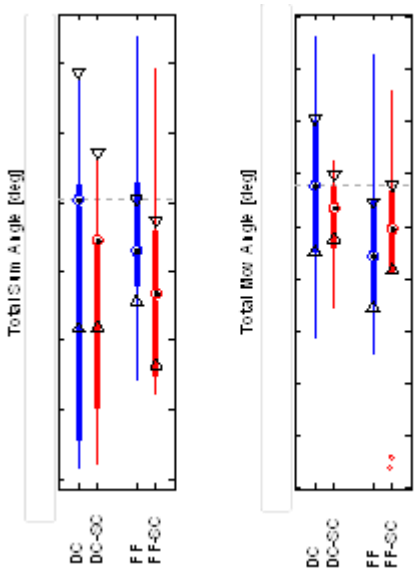

Figure 60: Statistical results of the average total sum angle and moving angle of both joystick angles, for all four experimental conditions.

None of the shown data in Figure 60 has a statistical significant different mean compared to the baseline condition (DC).

4.3.2 Catch Trial of Hard Soil

During this catch trial, very hard soil conditions were applied for the virtual slave robot simulation, exceeding the grab's capabilities. A reduced number of performance, system data and control effort results are given, due to some irrelevant metrics for this catch trial.

Performance and System Results

The results of time to complete the task and maximum heeling angle of the grabs frame are given in Figure 61. The evaluation metric production is not shown for this catch trial, because no gained volume was possible with these soil conditions. The results do not show a clear indication of changed reactions for this trial using different feedback mechanisms.

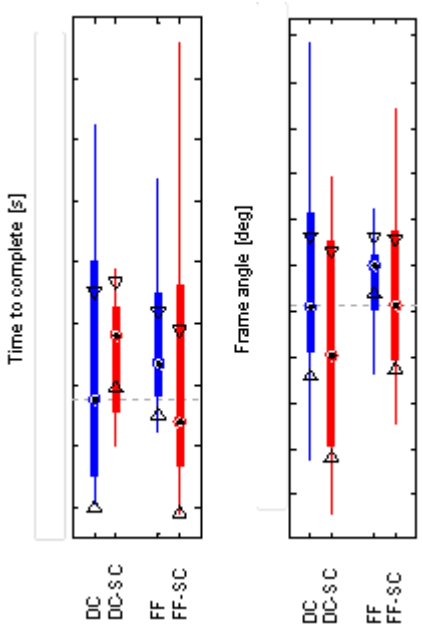

Figure 61: Statistical results for the time to complete the task and maximal heeling angle of the grabs frame, for all four experimental conditions.

None of the shown data in Figure 61 has a statistical significant different mean compared to the baseline condition (DC).

Control Effort Results

Statistical results of the control effort of the joystick angles for the catch trial with hard soil are shown Figure 62, which is similar to Figure 60 of the catch trial of a critical situation.

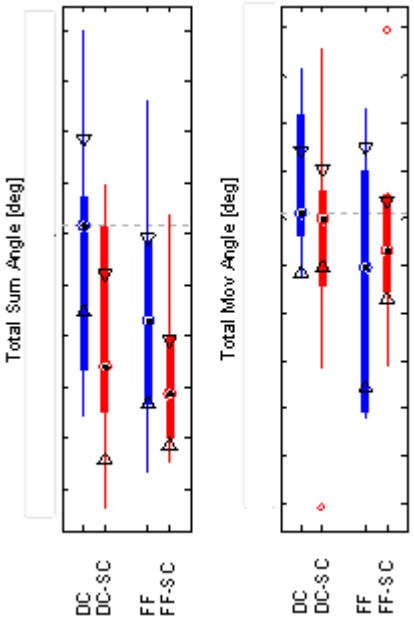

Figure 62: Statistical results of the average total sum angle and moving angle of both joystick angles, for all four experimental conditions.

The difference of the results shown in Figure 62 to the critical situation is that most of these results do show a statistical difference in reduction of control effort, as listed in Table 21.

Condition	Total Sum Angle	Total Mov Angle
DC : DC-SC	•	-
DC : FF	•	•
DC : FF-SC	••	-
DC-SC : FF-SC	-	-
FF : FF-SC	•	-

Table 21: Two-way ANOVA results of control effort data for the catch trial of hard soil, using (••) for p≤0.01, (•) for p≤0.05 and (-) for p>0.05 significance level.

4.3.3 Catch Trial of Reaction Time

This catch trial consisted of a mechanical failure during operation of the task with normal soil conditions, as described in paragraph 2.1.3. Statistical results of the reaction time to this failure are shown in Figure 63 for all four experimental conditions. A slight decrease for natural force feedback mechanism (FF) is shown, compared to the baseline condition (DC). The spread in data is very large because of the small sample size.

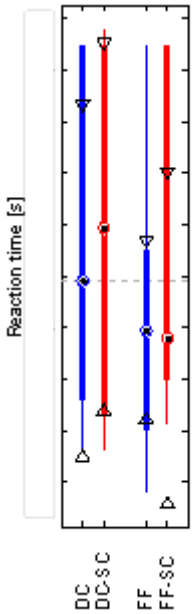

Figure 63: Statistical results of the reaction times to mechanical failure during the catch trial, shown for all four experimental conditions.

None of the shown data in Figure 63 has a statistical significant different mean compared to the baseline condition (DC).

5 DISCUSSION

Controlling a deep sea mining process to excavate SMS deposits of the seafloor by teleoperation is a complex procedure and has not been done so far. A promising way for excavation is the use of a large hydraulic grab, suspended from a ship as described in paragraph 1.1.1, using hydraulic actuators as described in paragraph 1.1.3. Controlling a suspended grab by teleoperation using a standard human-machine interface with only visual feedback is difficult for the human operator (Es 2004 [10]). Literature describes two types of haptic feedback mechanisms to improve the human-machine interface for controlling the deep sea mining excavation process, natural force feedback as described in paragraph 1.2.1 and haptic shared control as described in paragraph 1.2.2. Both methods have shown improvements for controlling a teleoperation for position control (FF, Wildenbeest et al. 2010 [39]; SC, Abbink 2006 [1], Abbink et al. 2008 [2], Boessenkool et al. 2011 [7]), however their usefulness is still unknown when applied on rate and force control when used for a deep sea mining process (Zhu and Salcudean 1995 [41]).

In this thesis an experimental setup is developed to determine the effect of haptic feedback mechanisms on the performance and effort of controlling a deep sea mining operation. The experiment consists of a human operator conducting a virtual deep sea mining task using two haptic joysticks and a display as shown in Figure 20 in chapter 2. The haptic joysticks of the experimental setup applied force feedback to the human operator with additional information to control the operation. The design of the haptic joysticks however appeared to have a relative short stroke for controlling the process compared to industrial joysticks, sometimes inducing non-continuous control. The relative short design of the joysticks was caused by the limiting motor torque of the given electric motors in combination with the given cable spring design. The information details of force feedback were therefore also more difficult to be noticed correctly due to the low feedback forces and short sticks. The conducted experiment consisted of six different tasks for every experimental condition. An extra set of experiments with one subject were conducted to determine if variation in outcome would be reduced when constantly conducting a single identical task instead of six different tasks. However the results had an unchanged outcome for conducting only identical tasks, indicating the task in general to be difficult to conduct due to the absence of a clear optimal control path.

Two types of tasks were conducted during the experiment to determine the effect of the haptic feedback conditions; performance tasks to determine the influence on the production and control effort, and catch trial tasks to determine the influence on critical parameters and reaction times. The general production results of the performance tasks as shown in Figure 46 and showed no difference for changing haptic feedback conditions. The reduction of the number of time penalties for incorrect control resulting in a critical control error, as shown in Figure 47, indicates an increase in situation awareness when offering natural force feedback. The time traces results as shown in Figure 48 and in paragraph 4.1.1, indicate the unclear optimal control path which occurred due to a lots of variation of control inputs for operating identical tasks under different conditions. These results also display the difficulty of operating the process with the small stroke joysticks, resulting in bang-bang control, as shown in Figure 48 a). The subjective results of the subjects' self-assessment showed a clear reduction in workload and increase in overall rating when applying haptic feedback mechanisms as shown in Figure 52. This indicates improvement of controlling the process even when production results did not show any change.

The production results of the performance trials as defined as time to complete and production volume, as shown in Figure 53 show hardly any statistical difference for varying conditions. However the control effort as shown in Figure 55 and Figure 56 for joystick angles does indicate a reduction when using haptic shared control conditions. The results of the catch trial for conducting a task in a critical situation displayed in Figure 59, showed reduction of the maximal heeling angle of the grab for natural force feedback conditions. This indicates an improvement of the situation awareness for applying transparency in the teleoperation. The reduction in control effort when applying haptic shared control for the critical situation catch trial as shown in

Figure 60, is much less in comparison with the performance trials. On the other hand the catch trial for hard soil conditions as shown in Figure 62 did indicate a reduction of control effort when applying haptic shared control. However the catch trial of hard soil as is displayed in Figure 61 did not show a reduction of time to complete, which would be a reasonable explanation for a reduction of control effort. The reaction time during the mechanical failure catch trial displayed in Figure 63 showed a slight improvement for natural force feedback, but which was not significant.

The summarised results of improved performance are listed in Table 22 and are compared with the hypothesis, based on production results during performance trials and catch trials. The effect as stated in the hypothesis for increase of performance is not measured, only during the difficult catch trials more production is measured when combining both haptic feedback mechanisms.

Performance	**No NFF**			**NFF**		
	HYP	PR-PT	PR-CT	HYP	PR-PT	PR-CT
No HSC	0	0	0	+	0	0
HSC	+	0	0	+	0	+

Table 22: Results summery of increase of performance for all conditions. In grey are stated the hypothesis and green the results validating the hypothesis, red indicated the hypothesis partly rejected (Hypothesis / Results). Results are given for the hypothesis (HYP), production during performance trials (PR-PT) and production during catch trials (PR-CT)

The summarized results of the reduced control effort are listed in Table 23 and are based on total summed control angle and high frequency movement of the joystick angle during performance trials. The results give an indication of the verification of the hypotheses when reduced control effort when offering haptic shared control.

Control Effort	**No NFF**				**NFF**			
	HYP	SUM	HF	WL	HYP	SUM	HF	WL
No HSC	0	0	0	0	0	0	0	+
HSC	+	+	0	0	+	+	+	+

Table 23: Results summery of reduction of control effort for all conditions during performance trials, given for the hypothesis (HYP), joystick summation angle (SUM), high frequency joystick angles (HF) and subjective workload (WL).

The summarised results of the improved situation awareness listed in Table 24, based on heeling angle at difficult conditions and reaction times to mechanical failures during catch trials. The results indicate the verification of the hypothesis for increased situation awareness for offering natural force feedback.

Situation Awareness	**No NFF**			**NFF**		
	HYP	ANG	RT	HYP	ANG	RT
No HSC	0	0	0	+	+	0
HSC	+	0	0	+	+	0

Table 24: Results summery of increase of situation awareness for all conditions during catch trials, given for the hypothesis (HYP), frame heeling angle (ANG) and reaction time to mechanical failure (RT).

In conclusion the experimental results indicate that haptic shared control does not seem to increase the performance of an operation. However it does reduce the control effort, resulting in a less demanding task for the operator and therefore the task is easier to complete. On the other hand natural force feedback showed improvements in situation awareness, resulting in less control errors during operation. This implies that human operators pay more attention to the process due to the short term increased situation awareness and long term less demanding tasks when both natural force feedback and haptic shared control are applied, which results in less errors causing production loss or damaging the system.

6 CONCLUSION

Derived from the experimental results it can be concluded that controlling a deep sea mining process can be improved by offering haptic feedback to the operator, thereby informing the environmental forces by offering natural force feedback and guiding the operator to an optimal control of the process by offering haptic shared control with attractive guiding forces.

The experimental results during normal task completion indicate an increase in situation awareness of the subject when natural force feedback was applied. This can be seen in a reduction of control errors resulting in a reduction of a critical heeling angle of the grab. Also the reaction time during a mechanical failure and the given time penalties for incorrect control were reduced when natural force feedback was applied. However the results of the experiment during a task at normal conditions did not show an increase in performance when applying haptic shared control. Also the results for time to complete the task or the gained production results did not show improvements. On the other hand the control effort did decrease for controlling a normal task and for conducting a difficult task. The subjective overall workload and overall rating results showed improvements for both feedback mechanisms.

To summarize the conclusions of this thesis the following statements can be made.

- Natural force feedback showed an increase in situation awareness, causing a reduction of critical heeling angle of the grab. It also showed a reduction of the reaction time during mechanical failure and a reduction of incorrect control resulting in critical situations.
- Haptic shared control showed no increase in performance at normal conditions, but did show a reduction of control effort at normal and difficult conditions.
- Combining natural force feedback and haptic shared control showed reduction of subjective workload and rating.

Therefore for this experiment it can be concluded that when controlling a deep sea mining tele-operation using rate and force control, offering natural force feedback improves the situation awareness and haptic shared control reduces the control effort of the human operator. However improvements of the operation performance were not found for either haptic feedback mechanisms. Nonetheless this implies that less production loss will occur due to incorrect control and damage of the system when combining the haptic feedback mechanisms for a deep sea mining tele-operation.

7 RECOMMENDATIONS

The described experiments did not completely give clear results for all situations, and only partly validated the hypotheses. Limitations of the experimental setup are partly the cause of these outcomes, therefore a list of recommendations is given for further experiments.

- It is recommended to use a different mechanical principle of actuating the joysticks as shown in Figure 64 a), thereby enabling high dynamic actuation and removing the limitations due to springs. By direct coupling of motor and joystick without springs it will enable higher actuation forces, not limited by the springs and removing backlash of the gearbox.

- Another suggestion would be to use longer handles of the mechanical setup as shown in Figure 64 b), for more control and sensitivity of forces. The downside of this is a larger required motor force, due to the increase momentum.

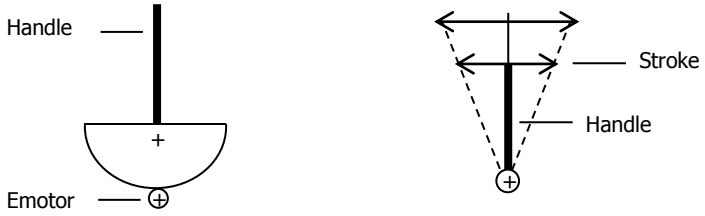

Figure 64: a) Schematic view of recommendation for improved design for mechanical principle of the experimental setup. b) Schematic view for improved dimensions of the experimental setup

- It is also recommended to use one ground model for all tasks to improve learning and to increase distinction between feedback methods, despite the fact that a quick look of this method did not show any mayor differences as previously described.

ABBREVIATIONS

ANOVA	:	ANalysis Of VAriance
DoF	:	Degree of Freedom
DC	:	Direct Control
DC-SC	:	Direct Control using haptic Shared Control feedback
DSS	:	Driver Support System
DUT	:	Delft, University of Technology
FF	:	natural Force Feedback
FF-SC	:	both natural Force Feedback with haptic Shared Control feedback
FRVF	:	Forbidden-Region Virtual Fixtures
MMI	:	Man-Machine Interface
SC	:	Shared Control feedback mechanism
SMS	:	Seafloor Massive Sulphides
SVI	:	Standard Variable Interface
TCP	:	Transmission Control Protocol
TLX	:	Task Load Index
VF	:	Virtual Fixtures
UIC	:	University of Illinois at Chicago
NOAA	:	National Oceanic and Atmospheric Administration
HMI	:	Human Machine Interface
EC	:	Experimental Condition
MD	:	Mental Demand
PD	:	Physical Demand
TD	:	Temporal Demand
PE	:	PErformance
EF	:	EFfort
FR	:	Frustration level
HYP	:	Hypotheses
PR-PT	:	PRoduction during Performance Trials
PR-CT	:	PRoduction during Catch Trials
SUM	:	SUMmation angle of joystick control
HF	:	High Frequency
WL	:	subjective Work Load
ANG	:	machine heeling ANGle
RT	:	Reaction Time
P1-3	:	Performance trials number 1 to 3
C1-3	:	Catch trails number 1 to 3

NOMENCLATURE

A_{valve}	:	Hydraulic valve area
A_{pipe}	:	Hydraulic pipe area
B	:	Bulk modulus
B_{fluid}	:	Hydraulic fluid bulk modulus

c_h, c_v	:	Horizontal and vertical damping coefficient
$d\theta$	:	Change of equilibrium angle
dL, dL_{cable}	:	Differential cable length
F	:	Force
F_I	:	Impact force
F_H, F_V	:	Horizontal and vertical force component
F_G	:	Resulting grab from clamshells
F_w	:	Resulting winch force
F_{vol}	:	Force of hydraulic actuator
F_{max}	:	Maximum force
F_l, F_r	:	Left and right cutting force
F_{min}	:	Minimal feedback force
$F_{required}$	:	Required feedback force?
F_{end}	:	End feedback force
F_{winch}	:	Winch force
F_{set}	:	Force setpoint
k_h, k_v	:	Horizontal and vertical spring coefficient
P_0	:	Initial hydraulic pressure
Q_{cyl}	:	Hydraulic cylinder inflow
Q_{vol}	:	Hydraulic inflow
Q_{pump}	:	Hydraulic pump flow
U_{vol}	:	Hydraulic fluid velocity
V_0	:	Hydraulic initial volume
V_{fluid}	:	Hydraulic fluid volume
V_{vol}	:	Hydraulic volume
X	:	Sideways movement of grab
Y	:	Forward movement of grab
Z	:	Vertical movement of grab
α	:	Clamshell angle relative to grab
ΔP	:	Hydraulic differential pressure
ΔV	:	Hydraulic differential volume
θ_{grab}	:	Grab joystick angle
θ_{winch}	:	Winch joystick angle
$\theta_{SC,winch}$	:	Shared control angle for the winch joystick
θ	:	Angle
θ	:	Pitch angle of grab
θ_{frame}	:	Frame heeling angle
$\theta_{LF,grab}$	:	Low frequent grab joystick control angle
$\theta_{HF,grab}$	:	High frequent grab joystick control angle
θ_{winch}	:	Winch joystick angle
$\theta_{LF,winch}$	:	Low frequent winch joystick control angle
$\theta_{HF,winch}$	:	Low frequent winch joystick control angle
$\theta_{vibrate}$	:	Joystick vibration angle
$\theta_{equalibrium}$	:	Equilibrium joystick angle
φ	:	Heeling angle of grab
ψ	:	Heading angle of grab

REFERENCES

[1] David A. Abbink. Neuromuscular analysis of haptic gas pedal feedback during car following. *Ph.D. Thesis TU Delft*, 2006.

[2] David A. Abbink, Erwin R. Boer, and Mark Mulder. Motivation for continuous haptic gas pedal feedback to support car following. *IV'08 Conference*, 2008.

[3] J.J. Abbott and A.M. Okamura. Virtual fixture architectures for telemanipulation. IEEE International Conference on Robotics and Automation, 2003

[4] Berk, L.J.M. van den, van den Berk Consultancy; Recources of the Sea; 2009 van den Berk Consultancy. 2009.

[5] Bettini, P. Marayong, S. Lang, A.M. Okamura, and G. Hager. Vision assisted control for manipulation using virtual fixtures. *IEEE Transactions on Robotics*, 2004.

[6] J.W. van Bloois, IHC Merwede, J.C.L. Frumau, Seatools bv.; Deep Sea Mining, The New Horizon for Dredging Technology; 2009, Offshore Technology Conference. 2009.

[7] H. Boessenkool, D. Abbink, C. Heemskerk, F.C.T. van der Helm. Haptic shared control improves tele-operated task performance towards performance in direct control. *World Haptics Conference (WHC), IEEE, pp. 433-438.* 2011

[8] G. A. V. Christiansson, R. Q. van der Linde, and F. C. T. van der Helm. The influence of teleoperator stiffness and damping on object discrimination. *IEEE TRANSACTIONS ON ROBOTICS, VOL. 24, NO. 5*, 2008.

[9] M.R. Endsley. Toward a Theory of Situation Awareness in Dynamic Systems. *Human Factors, Vol. 37, No. 1, pp. 32-64.* 1995

[10] B. van Es, N. Pille, R. de Vlaming, and J. de Vries. Construction of wellhead protection glory holes for white rose project, Canada. *Terra et Aqua, No. 95, pp. 22-32.* 2004.

[11] H.F. George, and A. Barber. What is bulk modulus and when is it important. Hydraulics and Pneumatics, Lubrizol Corp., Penton Media, Inc., System Design pp. 34-39. 2007

[12] Weston B. Griffin, William R. Provancher, and Mark R. Cutkosky. Feedback strategies for shared control in dexterous telemanipulation. *Intelligent Robots and Systems Conference*, 2003.

[13] B. Hannaford. A Design Framework for Teleoperators with Kinesthetic Feedback. IEEE Transactions on Robotics and Automation, Vol. 5, No. 4, pp. 426-434. 1989.

[14] B. Hannaford, Stability and Performance Tradeoffs in Bi-Lateral Telemanupulation. *Proceedings, 1989 International Conference on Robotics and Automation, pp. 1764-1767.* 1989.

[15] B. Hannaford, L. Wood, D.A. McAffee, and H. Zak. Performance evaluation of a six-axis generalized force-reflecting teleoperator. *IEEE Trans. Syst., Man, Cybernetics.* 1991.

[16] S.G. Hart, and L. E. Staveland. Development of NASA-TLX (Task Load Index): Results of empirical and theoretical research. *Human Mental Workload*, 139-183 Elsevier Science. 1988.

[17] S. Hayati and S.T. Venkataraman. Design and implementation of a robot control system with traded and shared control capability. *IEEE International Conference on Robotics and Automation, p. 1310-1315*, 1989.

[18] P. Hoagland, S. Beaulieu, M.A. Tivey, R.G. Eggert, C. German, L. Glowka, and J. Lin. Deep sea mining of seafloor massive sulfides. *Marine Policy, Elsevier Ltd.*, 2009.

[19] N. Hogan. Impedance Control: An Approach to Manipulation. *IEEE, American Control Conference, pp. 304-313.* 1984

[20] K. Kaneko, H. Tokashiki, K. Tanie, and K. Komoriya. Impedance shaping based on force feedback bilateral control in macro-micro teleoperation system. *IEEE International Conference on Robotics and Automation*, 1997.

[21] D.A. Lawrence. Stability and transparency in bilateral teleoperation. *IEEE Trans. on Robotics and Automation vol 9. no 5. pp. 624-637*, 1993.

[22] I. Lipton. Mineral resource estimate solwara 1 project bismarck sea papua new guinea. *Golder Associates Pty Ltd*, 2008.

[23] R. McGill, J.W. Tukey, and W.A. Larsen. Variations of Box Plots. *The American Statistician, February 1978, Vol. 32, No 1, pp. 12-16.* 1978.

[24] P. Milgram, A. Rastogi, and J.J. Grodsk. Telerobotic control using augmented reality. *IEEE International Workshop on Robot and Human Communication*, 1995.

[25] M. Mulder, D. A. Abbink, and E. R. Boer. The effect of haptic guidance on curve negotiation behavior of young, experienced drivers. *Conference Proceedings - IEEE International Conference on Systems, Man and Cybernetics, pp. 804–809.* 2008

[26] G. Niemeyer and J. E. Slotine. Stable adaptive teleoperation. *IEEE Journal of Oceanic Engineering vol. 16*, 1991.

[27] S. Petersen and M.D. Hanningron. Modern seafloor massive sulfide deposits: Distribution, types of deposits and origin. *Leibniz-Institute of Marine Sciences, Deep-Sea Minerals and Mining Conference 2008*, 2008.

[28] R. Prada and S. Payandeh. On study of design and implementation of virtual fixtures. Virtual Reality, 13(2), 117-129, 2009.

[29] L.B. Rosenberg. The use of virtual fixtures as perceptual overlays. *Technical Report, Armstrong Laboratory*, 1992.

[30] C.P. Sayers, and R.P. Paul. An operator interface for teleprogramming employing synthetic fixtures. *Presence Cambridge Mass, Vol. 3, Issue 4, pp. 309-320.* 1994

[31] C.P. Sayers, R.P. Paul, L.L. Withcomb, and D.R. Yoerger. Teleprogramming for Subsea Teleoperation Using Acoustic Communication. *IEEE Journal of Oceanic Engineering, Vol 23, No. 1, pp. 60-71.* 1998

[32] S.D. Scott. Lessons from land for modern seafloor volcanogenic massive sulfides. *Scotiabank Marine Geology Research Laboratory, Deep-Sea Minerals and Mining Conferenece 2008*, 2008.

[33] T.B. Sheridan. Telerobotics. *IFAC World Congress, Munich*, 1989.

[34] M.K. Tivey. Generation of seafloor hydrothermal vent fluids and associated mineral deposits. *Oceanography 20, 1: pp. 50-65*, 2007.

[35] R. Tomovic. On man-machine control. *Automatica Vol 5. pp 401-404*, 1969.

[36] G.E. Totten. Handbook of Hydraulic Fluids Technology. CRC Press, 1999

[37] S.A. Trebilcock. Development of world's first seafloor massive sulphide mining system. *Nautilus Minerals Inc., Deep-Sea Minerals and Mining COnference 2008*, 2008.

[38] M.L. Turner, R.P. Findley, W.B. Griffin, M.R. Cutkosky, and D.H. Gomez. Development and testing of a telemanipulation system with arm and hand motion. *ASME Dynamic Systems and Control Division. pp. 1-7*, 2000.

[39] J.G.W. Wildenbeest, D.A. Abbink, C.J.M. Heemskerk, F.C.T. van der Helm. Improving the Quality of Haptic Feedback Yields Only Marginal Improvements in Teleoperated Task Performance. *Msc thesis, Delft Universisty of Technology.* 2010

[40] Y. Yokokohji, and T. Yoshikawa. Bilateral Control of Master-Slave Manipulators for Ideal Kinesthetic Coupling. Proceedings of the IEEE Conference on Robotics and Automation, pp. 849-858. 1992.

[41] M. Zhu and S.E. Salcudean. Achieving transparency for tele-operator systems under position and rate control. *International Conference on Intelligent Robots and Systems*, 1995.